Accepted Manuscript

Hydrazinyl arylthiazole based pyridine scaffolds: Synthesis, structural characterization, *in vitro* α-glucosidase inhibitory activity, and *in silico* studies

Farman Ali, Khalid Mohammed Khan, Uzma Salar, Muhammad Taha, Nor Hadiani Ismail, Abdul Wadood, Muhammad Riaz, Shahnaz Perveen

PII: S0223-5234(17)30487-7

DOI: 10.1016/j.ejmech.2017.06.041

Reference: EJMECH 9536

To appear in: *European Journal of Medicinal Chemistry*

Received Date: 3 April 2017

Revised Date: 3 June 2017

Accepted Date: 23 June 2017

Please cite this article as: F. Ali, K.M. Khan, U. Salar, M. Taha, N.H. Ismail, A. Wadood, M. Riaz, S. Perveen, Hydrazinyl arylthiazole based pyridine scaffolds: Synthesis, structural characterization, *in vitro* α-glucosidase inhibitory activity, and *in silico* studies, *European Journal of Medicinal Chemistry* (2017), doi: 10.1016/j.ejmech.2017.06.041.

Hydrazinyl arylthiazole based pyridine scaffolds: Synthesis, structural characterization, *in vitro* α-glucosidase inhibitory activity, and *in silico* studies

Farman Ali,[a] Khalid Mohammed Khan,[a] Uzma Salar,[a] Muhammad Taha,[b,c] Nor Hadiani Ismail,[b] Abdul Wadood,[d] Muhammad Riaz[d] and Shahnaz Perveen,[e]

[a]*H. E. J. Research Institute of Chemistry, International Center for Chemical and Biological Sciences, University of Karachi, Karachi-75270, Pakistan*

[b]*Atta-ur-Rahman Institute for Natural Product Discovery, Universiti Teknologi MARA (UiTM), Puncak Alam Campus, 42300 Bandar Puncak Alam, Selangor D. E. Malaysia*

[c]*Faculty of Applied Science Universiti Teknologi MARA, Shah Alam 40450, Selangor D. E., Malaysia*

[d]*Department of Biochemistry, Computational Medicinal Chemistry Laboratory, UCSS, Abdul Wali Khan University Mardan, Pakistan*

[e]*PCSIR Laboratories Complex, Karachi, Shahrah-e-Dr. Salimuzzaman Siddiqui, Karachi-75280, Pakistan*

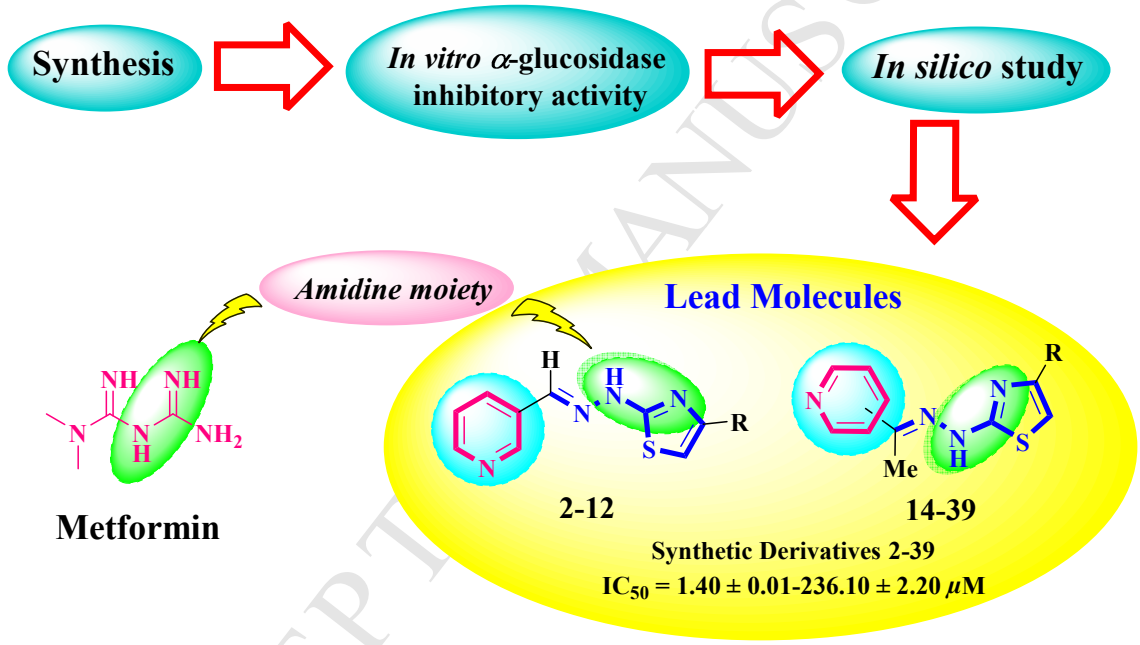

Hydrazinyl arylthiazole based pyridine scaffolds: Synthesis, structural characterization, *in vitro* α-glucosidase inhibitory activity, and *in silico* studies

Farman Ali,[a] Khalid Mohammed Khan,[a*] Uzma Salar,[a] Muhammad Taha,[b,c] Nor Hadiani Ismail,[b] Abdul Wadood,[d] Muhammad Riaz,[d] and Shahnaz Perveen,[e]

[a]*H. E. J. Research Institute of Chemistry, International Center for Chemical and Biological Sciences, University of Karachi, Karachi-75270, Pakistan*
[b]*Atta-ur-Rahman Institute for Natural Product Discovery, Universiti Teknologi MARA (UiTM), Puncak Alam Campus, 42300 Bandar Puncak Alam, Selangor D. E. Malaysia*
[c]*Faculty of Applied Science Universiti Teknologi MARA, Shah Alam 40450, Selangor D. E., Malaysia*
[d]*Department of Biochemistry, Computational Medicinal Chemistry Laboratory, UCSS, Abdul Wali Khan University Mardan, Pakistan*
[e]*PCSIR Laboratories Complex, Karachi, Shahrah-e-Dr. Salimuzzaman Siddiqui, Karachi-75280, Pakistan*

Abstract: Acarbose, miglitol, and voglibose are the inhibitors of α-glucosidase enzyme and being clinically used for the management of type-II diabetes mellitus. However, many adverse effects are also associated with them. So, the development of new therapeutic agents is an utmost interest in medicinal chemistry research. Current study is based on the identification of new α-glucosidase inhibitors. For that purpose, hydrazinyl arylthiazole based pyridine derivatives **1-39** were synthesized *via* two step reaction and fully characterized by spectroscopic techniques EI-MS, HREI-MS, ^{1}H-, and ^{13}C-NMR. However, stereochemistry of the iminic bond was confirmed by NOESY. All compounds were subjected to *in vitro* α-glucosidase inhibitory activity and found many folds active (IC_{50} = 1.40 ± 0.01-236.10 ± 2.20 μM) as compared to the standard acarbose having IC_{50} value of 856.45 ± 5.60 μM. A limited structure-activity relationship was carried out in order to make a presumption about the substituent's effect on inhibitory activity which predicted that substituents of more negative inductive effect played important role in the activity as compared to the substituents of less negative inductive effect. However, in order to have a good understanding of ligand enzyme interactions, molecular docking study was also conducted. *In silico* study was confirmed that substituents like halogens (Cl) and nitro (NO_2) which have negative inductive effect were found to make important interactions with active site residues.

[*]*Corresponding Author*: khalid.khan@iccs.edu; drkhalidhej@gmail.com; Tel. 00922134824910; Fax. 00922134819018

Keywords: Synthesis; pyridine; hydrazinyl arylthiazole; *α*-glucosidase; *in vitro*; structure-activity relationship; molecular docking.

Introduction

Type-II diabetes mellitus is responsible for around 5% death of global population. *α*-Glucosidase enzyme catalyzes the hydrolysis of *α*-glucosidal bond of complex carbohydrates and releases the monosaccharide (*α*-D-glucose) which is absorbable in small intestine [1,2]. Hyperactivity of *α*-glucosidase enzyme resulted in elevated level of blood glucose in diabetic patients and termed as hyperglycemia [3]. Inhibition of *α*-glucosidase enzyme is one way to treat type-II diabetes mellitus by suspending the absorption of glucose in intestine [4]. Acarbose, miglitol, and voglibose are the drugs which are being clinically used for the treatment of type-II diabetes mellitus (Figure-1). These all are the inhibitors of *α*-glucosidase enzyme [5,6] but 50% less effective than the other anti-diabetic drugs such as metformin and sulfonylurea. However, adverse effects are also linked to them such as abdominal discomfort, diarrhea, and flatulence [7]. Therefore, these medications are often use in combination with other anti-diabetic agents to improve the effectiveness. So, it is still an interest in medicinal chemistry to develop a safer medication to cure diabetes mellitus.

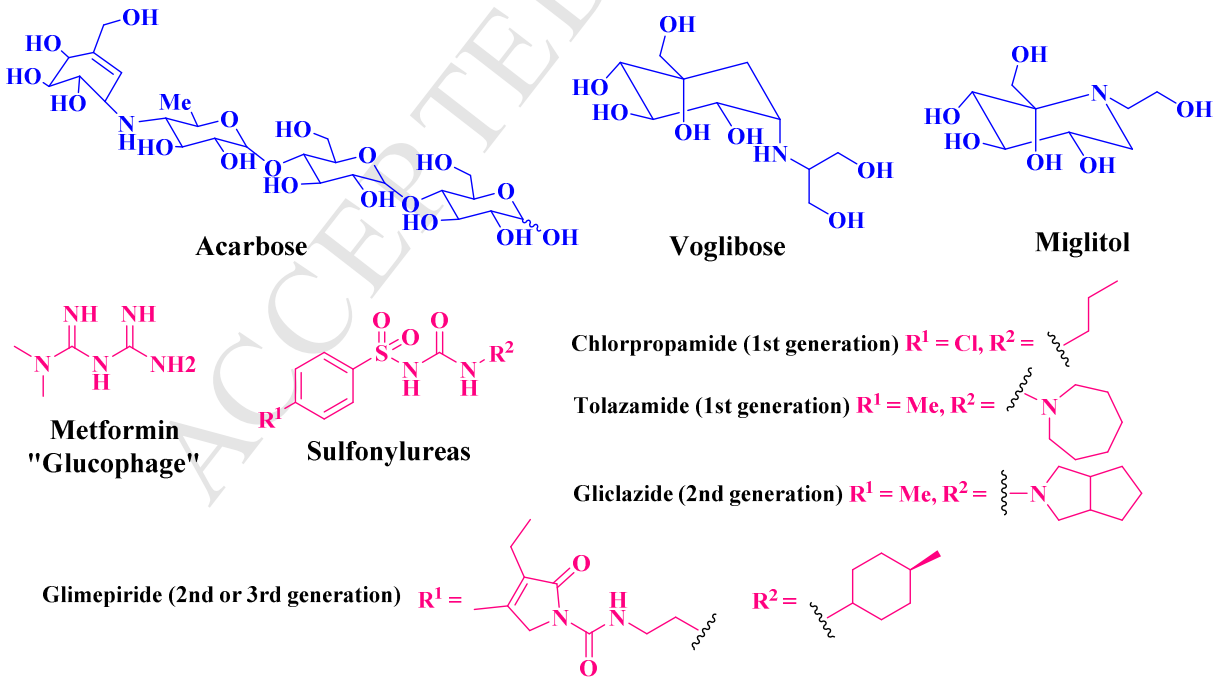

Figure-1: Clinical drugs for type II diabetes mellitus

Heterocyclic rings are the basic motifs of various biologically active compounds and natural products [8-11] and have received much attention in drug discovery and lead optimization [12]. Specially, nitrogen-containing heterocycles have lots of applications in pharmaceuticals, agrochemicals, and functional materials [13-14]. As far as pyridine is concerned, it is the basic part of many natural products such as vitamin B_3, coenzyme vitamin B_6 family, and various alkaloids. These natural products exhibit many interesting biological activities [15-17]. Polysubstituted pyridines have been used as antiprion, antibacterial, and anticancer agents. These were also used as potassium channel openers for the cure of urinary incontinence [18-20]. Furthermore, some derivatives were aslo found to be highly selective ligands for adenosine receptors [21], a potential targets for the identification of new drugs to treat Parkinson's disease, asthma, hypoxia/ischaemia, kidney diseases, and epilepsy [22]. Thiazole ring is the core scaffold of medicinally important compounds [23] and possess significant biological potential such as anticonvulsant, antiinflammatory, analgesic, antituberculosis, antiviral, pesticidal, antimicrobial, anticancer, antitumor, and enzyme inhibition activities [24-32].

There are many reports available on the *α*-glucosidase inhibitory activity of isolated natural products such as monoterpenoids, triterpenes, sesquiterpenoids, isoindolin-1-ones, *p*-terphenyl scaffolds [33-37]. Our group has identified many heterocyclic compounds having promising *α*-glucosidase inhibitory activity (Figure-2) [38-43]. Figure-3 displayed that the new synthetic compounds have structural resemblance such as pyridine ring, thiazole ring and hydrazine moiety, with the already identified lead candidates (Figure-2) which prompted us to screen these hybrid scaffolds for *α*-glucosidase inhibitory potential. It is worth-mentioning that synthetic compounds also have the same amidine moiety as in the antidiabetic agent "metformin" (Figure-3).

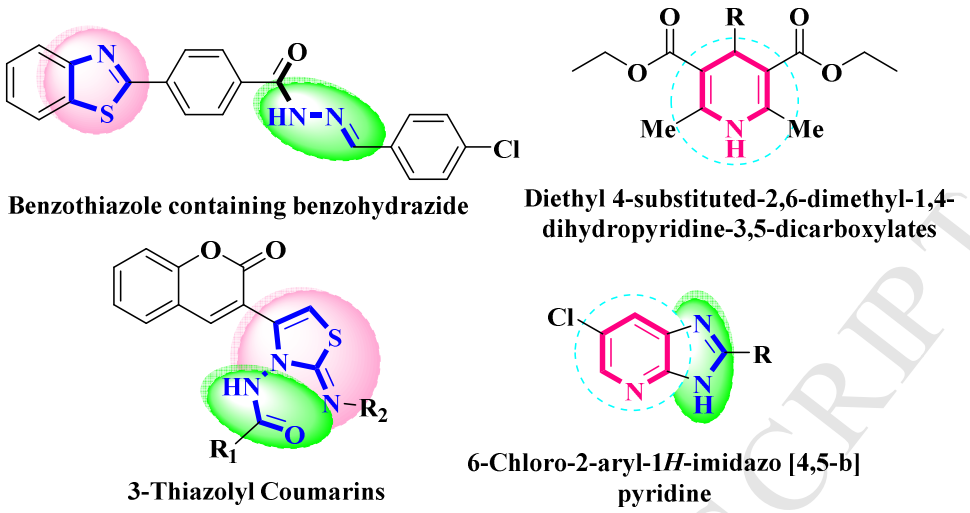

Figure-2: Identified leads for *α*-glucosidase inhibitory activity

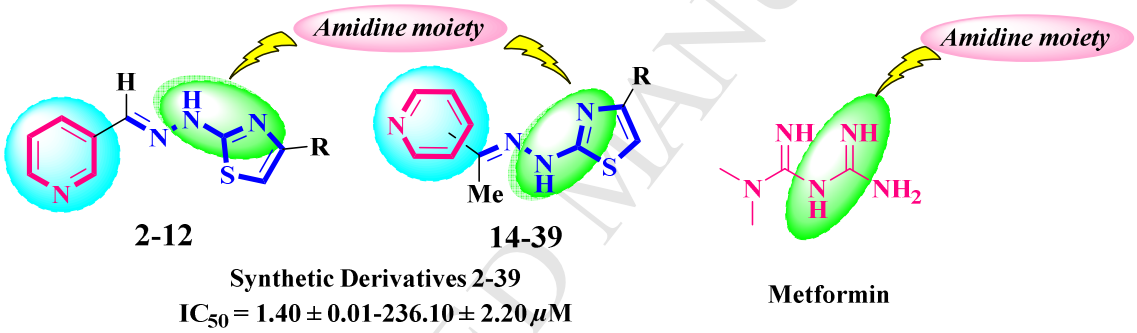

Figure-3: Rationale of the Current Study

This manuscript described the synthesis, structural characterization, *in vitro* inhibition, and *in silico* studies of arylated hydrazinyl thiazole based pyridine derivatives **1-39** as well as identification of lead compounds against the *α*-glucosidase enzyme for the treatment of type-II diabetes mellitus.

Results and Discussion

Chemistry

Arylated hydrazinyl thiazole based pyridine derivatives **1-39** were synthesized *via* two steps reaction scheme. In the first step, 3-pyridinecarboxaldehyde or 2/3/4-acetylpyridine was treated with thiosemicarbazide to afford thiosemicarbazone intermediates (**1**, **13**, **22**, and **31**). Catalytic

amount of glacial acetic acid was used in the reaction. In second step thiosemicarbazone intermediates (**1**, **13**, **22**, and **31**) undergo the cyclization reaction with substituted phenacyl bromides to form thiazole ring *via* Hantzsch reaction (Scheme-1). Reaction progress was checked by thin layer chromatography (TLC). After completion of the reaction, flask was kept overnight at room temperature to afford precipitates. Resulting precipitates were washed with distilled water and crystallized from ethanol to afford the pure products. Purity of compounds were checked *via* TLC analysis. Spectroscopic techniques EI-MS, HREI-MS, ^{1}H-, and ^{13}C-NMR were used to characterize the structures of synthetic compounds **1-39** (Table-1). However, 2D-NMR (COSY, HSQC, HMBC, and NOESY) of representative and structurally new compound **18** was also carried out.

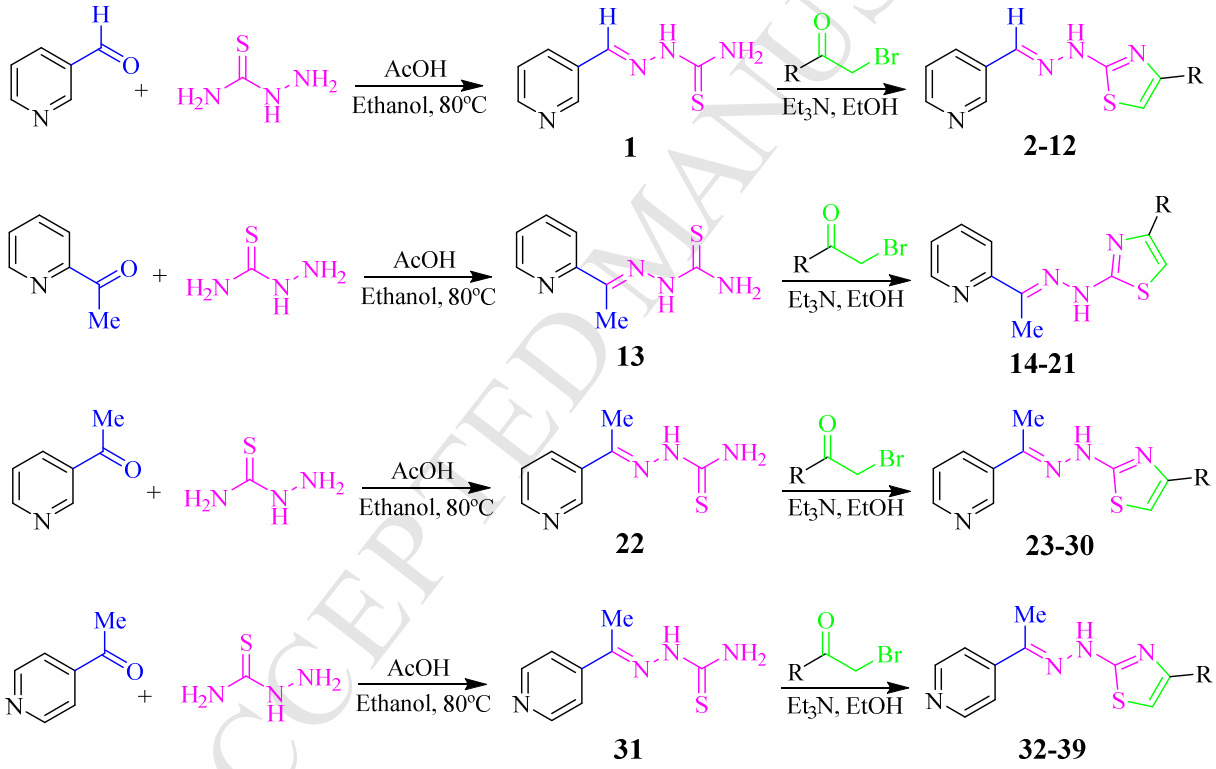

Scheme-1: Synthesis of hydrazinyl thiazole based pyridine derivatives **1-39**

Characteristic spectral feature of representative compound 18

^{1}H- and ^{13}C-NMR spectra of compound **18** were recorded in DMSO-d_6. In ^{1}H-NMR spectrum, the most downfield broad singlet of the NH which is directly attached to thiazole skeleton,

appeared at δ_H 11.47. Another downfield signal of H-6 of pyridine skeleton was appeared at δ_H 8.58 (d, $J_{6,5}$ = 4.4 Hz), showed *ortho* coupling with H-5. Downfield chemical shift is due to the presence of more electronegative nitrogen atom at *ortho* position. H-3 of pyridine skeleton was appeared in downfield region at δ_H 8.03 (d, $J_{3,4}$ = 8.4 Hz), showed *ortho* coupling with H-4. A singlet of H-2″ was appeared at δ_H 7.93. Signals of two protons H-4 and H-6″ were overlapped and appeared at δ_H 7.85. The characteristic singlet of H-5' of thiazole moiety was appeared at δ_H 7.60. H-5 was appeared as a triplet at 7.46 (t, $J_{5(4,6)}$ = 8.0 Hz). Signals of two H-4″, H-5″ overlapped and appeared at δ_H 7.37. The protons of iminic methyl was appeared as a singlet at δ_H 2.40 (Figure-4).

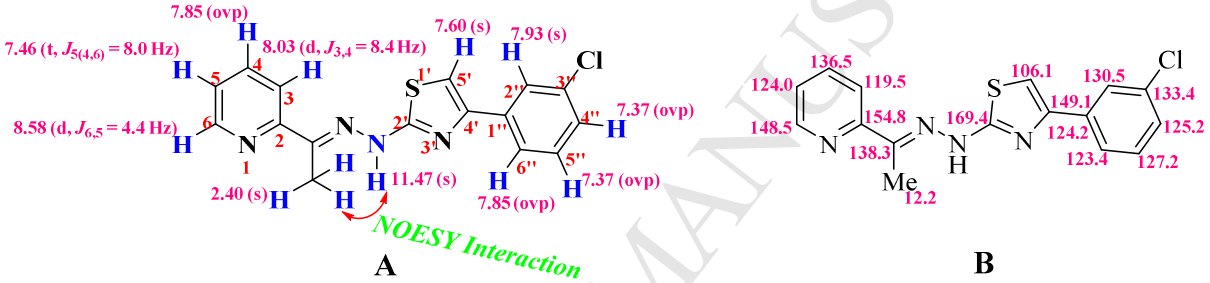

Figure-4: ^{1}H-NMR and ^{13}C-NMR chemical shifts of compound **18**

^{13}C-NMR broad-band decoupled spectrum displayed total sixteen carbon signals, including six quarternary, nine methine, and one methyl carbons. The quaternary carbon of thiazole ring, attached to the more electronegative nitogen and sulfur atoms, was the most downfield signal and appeared at δ_C 169.4. The second most downfield signal was the quaternary C-2 of pyridine ring which is lying adjacent to nitrogen and imine bond and appeared at δ_C 154.8. The quaternary C-4′ of thiazole and CH-6 of pyridine ring which are directly attached to electronagative nitrogen atom, were resonated at δ_C 149.1 and δ_C 148.5, respectively. The quaternary carbon of imine was resonated at δ_C 138.3. Two quaternary carbons of phenyl C-3″ and C-1″ were resonated at δ_C 133.4 and δ_C 124.2, respectively. Four aromatic methine carbons (CH-2″, CH-4″, CH-5″, and CH-6″) and three methine carbons of pyridine ring (CH-3, CH-4, and CH-5) were appeared in the usual aromatic region δ_C 136-119. While characteristic C-5′ of thiazole ring was resonated at δ_C 106.1. The most upfield iminic methyl was appeared at δ_C 12.2 (Figure-4).

The $^{13}C/^{1}H$-NMR chemical shifts were assigned on the basis of COSY, HSQC, and HMBC correlations. Stereochemistry of the imine group (C=N) was found as *E*-configuration after analyzing the NOESY spectrum in which iminic methyl protons (CH_3-C=N) showed NOESY interaction with the NH (Figure-4).

EI-MS of compound **18** showed the molecular ion peak $[M]^+$ at *m/z* 328 and isotopic peak $[M+2]^+$ at *m/z* 330 in a ratio of 3:1 which confirmed the presence of chlorine atom. HREI-MS of compound **18** displayed M^+ at *m/z* 328.0544 with a composition of $C_{16}H_{13}ClN_4S$ (Calcd. 328.0549) which confirmed the formation of the desired molecule. However, the key fragmentation pattern obeserved in the spectrum showed that molecular ion undergo cleavage by three ways (**a**-**c**).

(a) Moleuclar ion M^+ at *m/z* 328 undergoes homolytic cleavage by the loss of methyl radical to yield a cation at *m/z* 313 which will further fragmented to yield another cation at *m/z* 223.

(b) In second way, moleuclar ion undergoes homolytic cleavage by the loss of pyridiyl radical to afford a cation at *m/z* 250 which is also the base peak in the spectrum.

(c) In third way, moleuclar ion undergoes complex series of homolytic cleavage to afford a radical cation at *m/z* 79 (Figure-5).

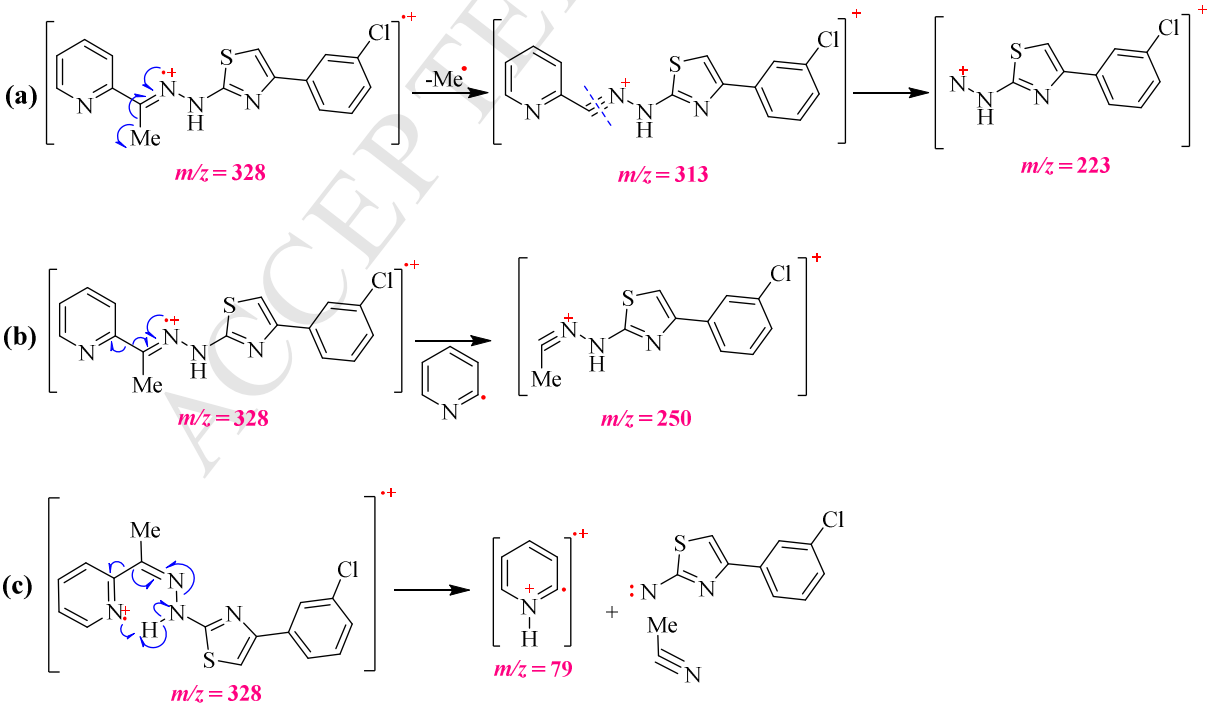

Figure-5: Key EI-MS fragmentation of compound **18**

***In vitro* α-glucosidase inhibitory activities**

All arylated hydrazinyl thiazole based pyridine derivatives **1-39** were screened to evaluate *in vitro* α-glucosidase inhibitory activity. All compounds demonstrated excellent and potent inhibitory activity in the range of IC_{50} = 1.40 ± 0.01-236.10 ± 2.20 μM as compared to the standard acarbose (IC_{50} = 856.45 ± 5.60 μM) (Table-1).

Table-1: *In vitro* α-glucosidase inhibitory activities of synthetic compounds **1-39**

Comp. No.	R	IC_{50} ± SEM[a] [μM]	Comp. No.	R	IC_{50} ± SEM[a] [μM]
Category "A"					
1	-	120.20 ± 1.10	**7**	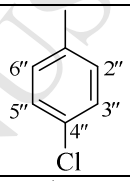	28.50 ± 0.25
2	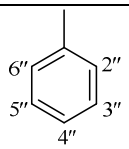	177.10 ± 1.10	**8**	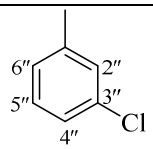	46.20 ± 0.40
3	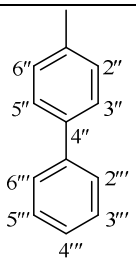	236.10 ± 2.20	**9**	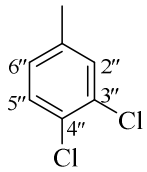	6.10 ± 0.01
4	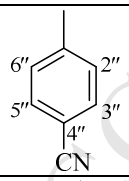	61.60 ± 0.50	**10**	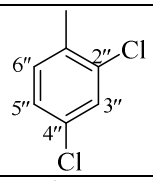	70.10 ± 0.68
5	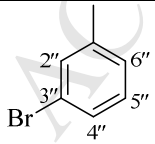	113.10 ± 1.10	**11**	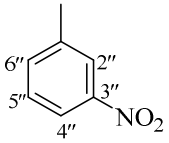	23.50 ± 0.20
6	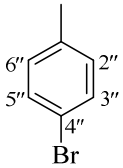	96.20 ± 0.80	**12**	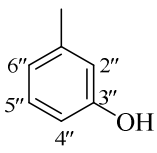	13.40 ± 0.10
Category "B"					

13	-	120.60 ± 1.10	**18**	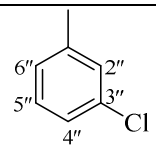	5.50 ± 0.10
14	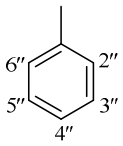	24.10 ± 0.24	**19**	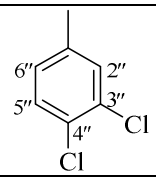	1.40 ± 0.01
15	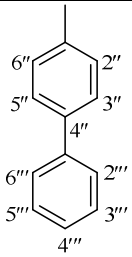	86.20 ± 0.80	**20**	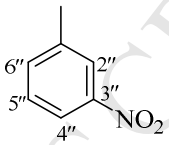	13.10 ± 0.15
16	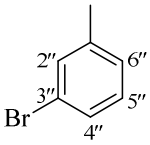	54.40 ± 0.60	**21**	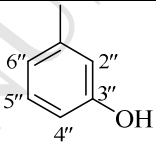	6.40 ± 0.10
17	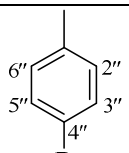	41.60 ± 0.45			
Category "C"					
22	-	86.40 ± 0.70	**27**	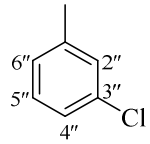	21.10 ± 0.20
23	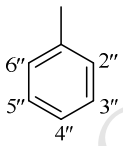	36.10 ± 0.30	**28**	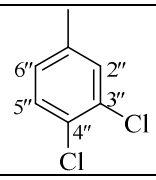	2.50 ± 0.01
24	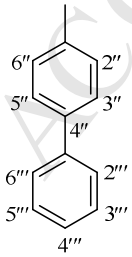	163.20 ± 1.40	**29**	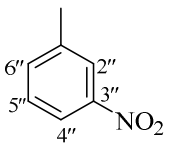	35.60 ± 0.35
25	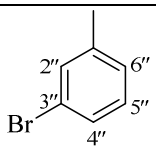	40.10 ± 0.40	**30**	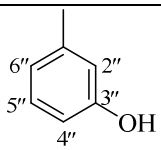	8.10 ± 0.10

26	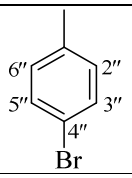	53.60 ± 0.50			
Category "D"					
31	-	115.50 ± 1.10	**36**	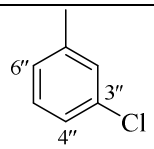	26.20 ± 0.24
32	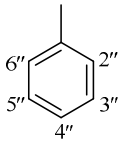	124.40 ± 1.20	**37**	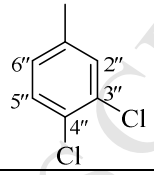	11.60 ± 0.15
33	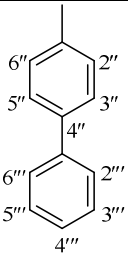	168.50 ± 1.40	**38**	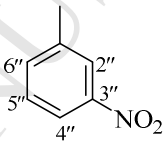	31.10 ± 0.30
34	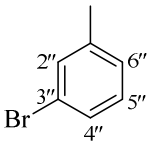	63.10 ± 0.55	**39**	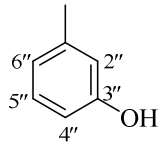	10.10 ± 0.10
35	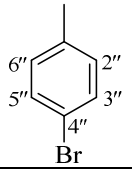	85.10 ± 0.80	Standard[c] = Acarbose		856.45 ± 5.60

[a]IC_{50} (mean ± standard error of mean); Standard[c] (Inhibitor for α-Glucosidase).

Structure-activity relationship (SAR)

Limited structure-activity relationship (SAR) was rationalized by observing the different substitution pattern at the aryl part (R). Although all constant structural features such as pyridine ring, thiazole ring, and Schiff base moiety are cordially playing their part in demonstrating the inhibitory potential, however, the varying features such as aryl ring "R" are responsible for variation in the inhibitory activity (Figure-6).

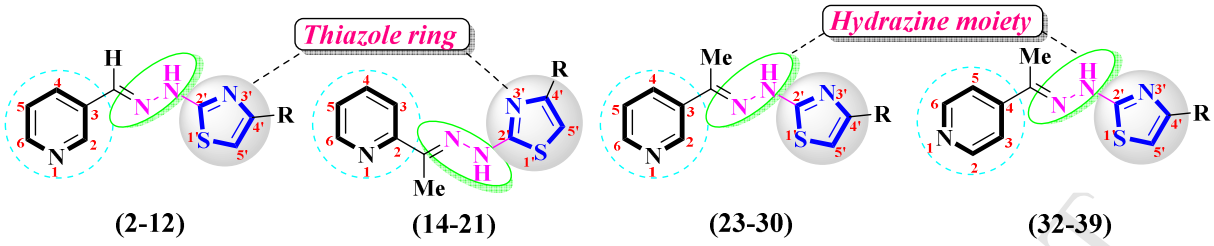

Figure-6: General structural features of synthetic compounds

For better understanding of structure-activity relationship, compounds were categorized into four categories "A-D", on the basis of four different thiosemicarbazone intermediates which are the precursors of rest of the cyclized products. Thiosemicarbazone intermediates such as **1** (IC_{50} = 120.20 ± 1.10 μM), **13** (IC_{50} = 120.60 ± 1.10 μM), and **31** (IC_{50} = 115.50 ± 1.10 μM) showed potent and comparable α-glucosidase inhibitory activity as compared to standard acarbose (IC_{50} = 856.45 ± 5.60 μM). Although intermediate **22** (IC_{50} = 86.40 ± 0.70 μM) showed more enhanced activity than intermediate **1** and positional isomers **22** and **31**. Might be the compound **22** attained the conformation which will better interact with the active site (Figure-7).

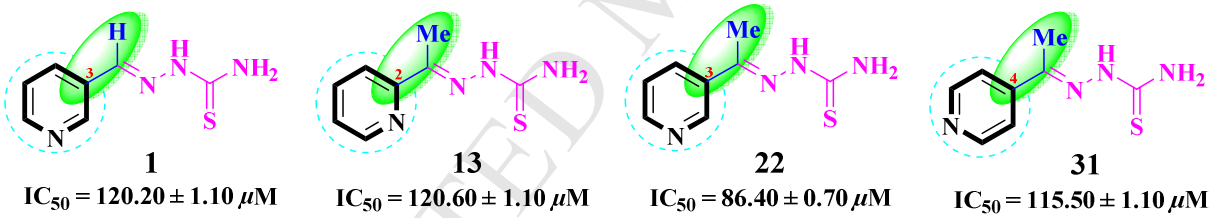

Figure-7: Structure-activity relationship of thiosemicarbazone intermediates 1, 13, 22, 31

Results depicted in Table-1 showed that most of the cyclized products displayed far better activity than thiosemicarbazone intermediates. All compounds **2-12** belongs to category "A" showed many folds enhanced activity in the range IC_{50} = 6.10-236.10 μM as compared to the standard acarbose (IC_{50} = 856.45 ± 5.60 μM). Compound **9** (IC_{50} = 6.10 ± 0.01 μM) with *m,p*-dichloro substitutions at aryl ring showed more than hundred folds better activity than standard acarbose. Its structurally similar compound **10** (IC_{50} = 70.10 ± 0.68 μM) with *o,p*-dichloro substitutions showed eleven times less activity than **9**. It shows that dichloro groups are playing a crucial part in the activity when present at *meta* and *para* positions. However, mono-chloro compounds **7** (IC_{50} = 28.50 ± 0.25 μM) and **8** (IC_{50} = 46.20 ± 0.40 μM) showed many folds

decreased activity as compared to dichloro compound **9** (Figure-8). It showed that number and positions of the substituent like chloro played an important role in exhibiting the inhibitory potential. Activity of compounds **7** (IC_{50} = 28.50 ± 0.25 μM) and **8** (IC_{50} = 46.20 ± 0.40 μM) can compared with compounds **6** (IC_{50} = 96.20 ± 0.80 μM) and **5** (IC_{50} = 113.10 ± 1.10 μM), respectively, having the bromo instead of chloro, about two fold decreased activity was observed. In case of compounds **11** (IC_{50} = 23.50 ± 0.20 μM) and **12** (IC_{50} = 13.40 ± 0.10 μM) having nitro and hydroxy groups, respectively, a better activity was observed. It was experienced that compounds with substituents having more negative inductive effect such as Cl, NO_2 and OH showed more potent inhibition than the compounds with less negative inductive effect (Figure-8).

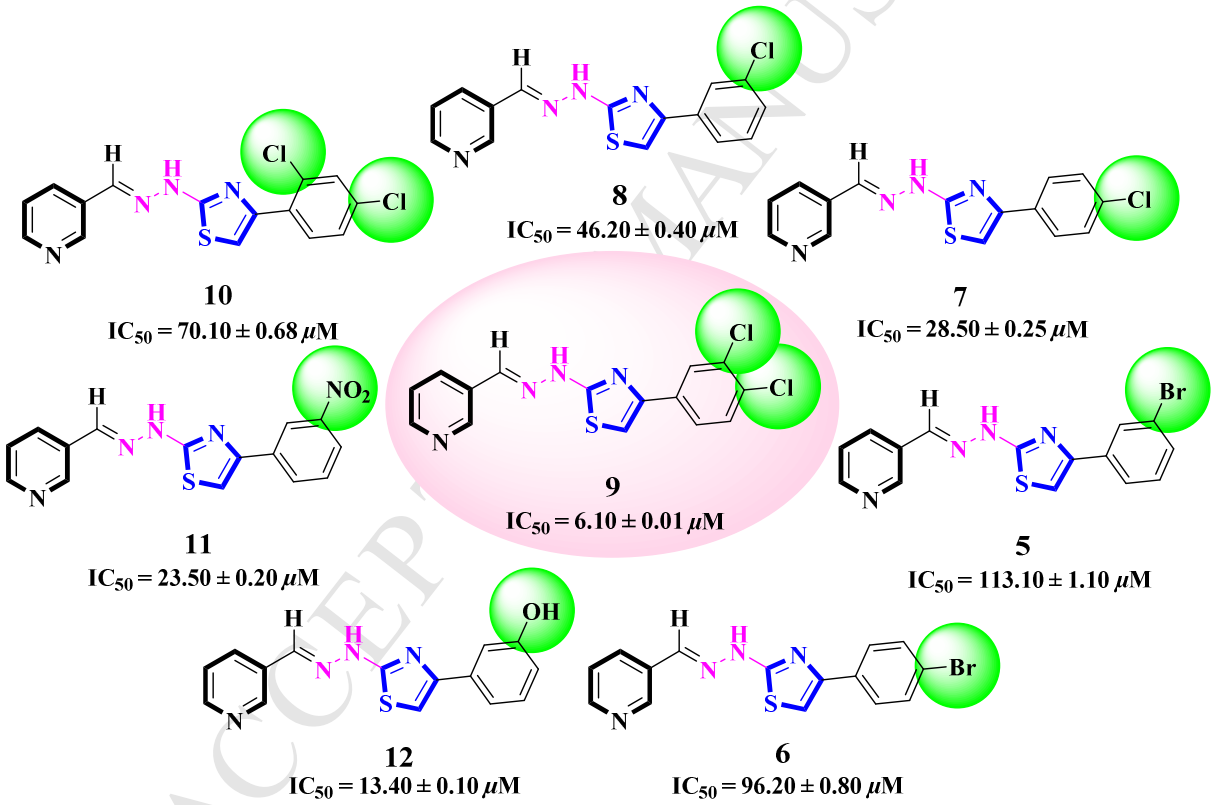

Figure-8: Structure-activity relationship of compounds 5-12

Similar activity trend was observed in the category "B" like category "A". *m,p*-Dichloro substituted analog **19** (IC_{50} = 1.40 ± 0.01 μM) was found to be the most active derivative of the whole series and six hundred times more active than the standard acarbose (IC_{50} = 856.45 ± 5.60

μM). Mono-chloro derivative **18** (IC_{50} = 5.50 ± 0.10 μM) was found to be less active than dichloro compound **19** (IC_{50} = 1.40 ± 0.01 μM). Similarly, bromo substituted compounds such as **16** (IC_{50} = 54.40 ± 0.60 μM) and **17** (IC_{50} = 41.60 ± 0.45 μM) showed less inhibitory activity. Compounds having substituents like OH and NO_2 such as compounds **20** (IC_{50} = 13.10 ± 0.15 μM) and **21** (IC_{50} = 6.40 ± 0.10 μM) demonstrated good inhibitory potential than the compound **14** (IC_{50} = 24.10 ± 0.24 μM) with no substitution and compound **15** (IC_{50} = 86.20 ± 0.80 μM) with biphenyl as R (Figure-9).

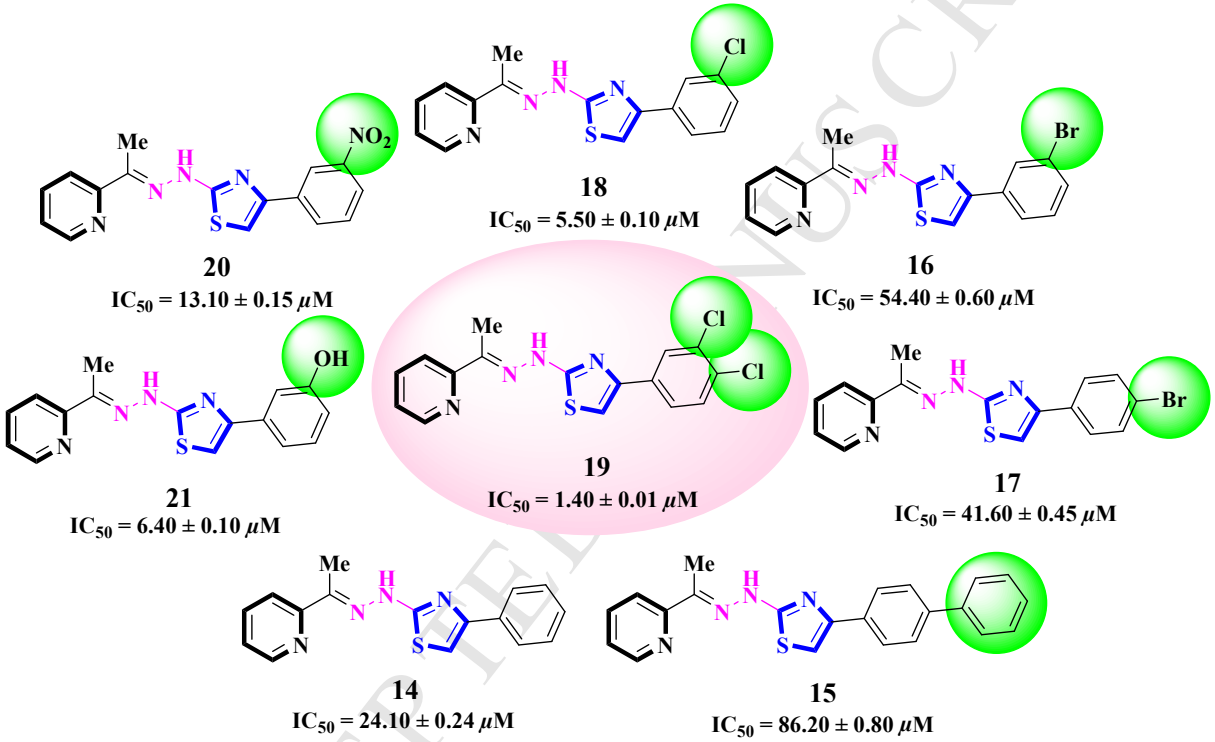

Figure-9: Structure-activity relationship of compounds 14-21

It is worth-noting that the most active derivative of category "C" was again found to be a dichloro analog **28** (IC_{50} = 2.50 ± 0.01 μM). Absence of chloro group at *para* position as in compound **27** (IC_{50} = 21.10 ± 0.20 μM) showed a decreased activity. Compound **30** (IC_{50} = 8.10 ± 0.10 μM) with the *m*-hydroxy substitution also showed potent inhibition. Switching of hydroxy to nitro group as in **29** (IC_{50} = 35.60 ± 0.35 μM), a decreased activity was observed. Similarly, bromo substituted compounds **25** (IC_{50} = 40.10 ± 0.40 μM) and **26** (IC_{50} = 53.60 ± 0.50 μM) were demonstrated less inhibition than hydroxy and nitro substituted derivatives. Compound **24** (IC_{50} = 163.20 ± 1.40 μM) with the biphenyl ring as "R" was found to be the least active among

category “C”. Least activity of biphenyl derivative might be either due to the increased carbon load or it is not fulfilling the conformational requirement to fit well in the active site (Figure-10).

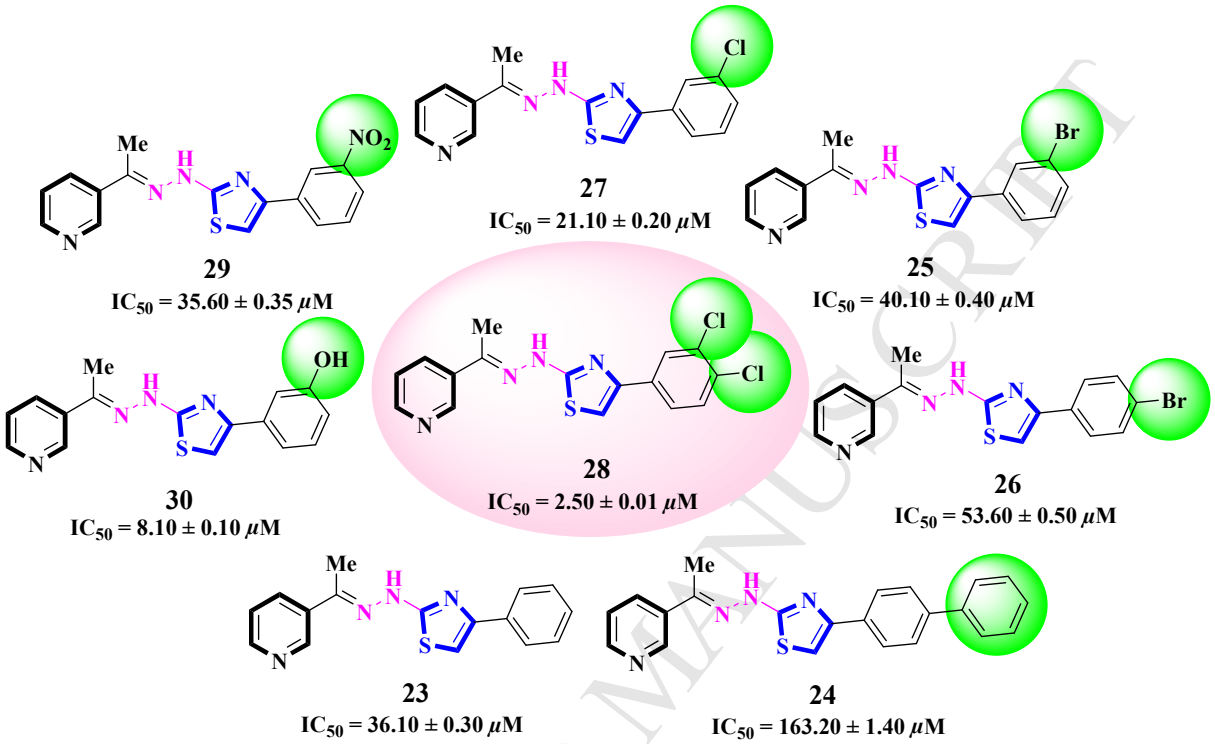

Figure-10: Structure-activity relationship of compounds 23-30

In case of category “D”, compound **39** (IC_{50} = 10.10 ± 0.10 μM) with *m*-hydroxy substitution was found to be the most active derivative and compound **37** (IC_{50} = 11.60 ± 0.15 μM) with *m,p*-dichloro substitutions was the second most active member of this category. Compound **26** (IC_{50} = 26.20 ± 0.24 μM) with *m*-chloro group showed less activity than dichloro analog. Switching from chloro to bromo group as in case of compounds **34** (IC_{50} = 63.10 ± 0.55 μM) and **35** (IC_{50} = 85.10 ± 0.80 μM), a less inhibition was experienced. Similarly, compound **38** (IC_{50} = 31.10 ± 0.30 μM) with *m*-nitro group also showed comparable activity with the most active compounds of this category. However, compound **32** (IC_{50} = 124.40 ± 1.20 μM) with no substitution and compound **33** (IC_{50} = 168.50 ± 1.40 μM) with biphenyl ring as “R”, were found to be least active analogs of this category (Figure-11).

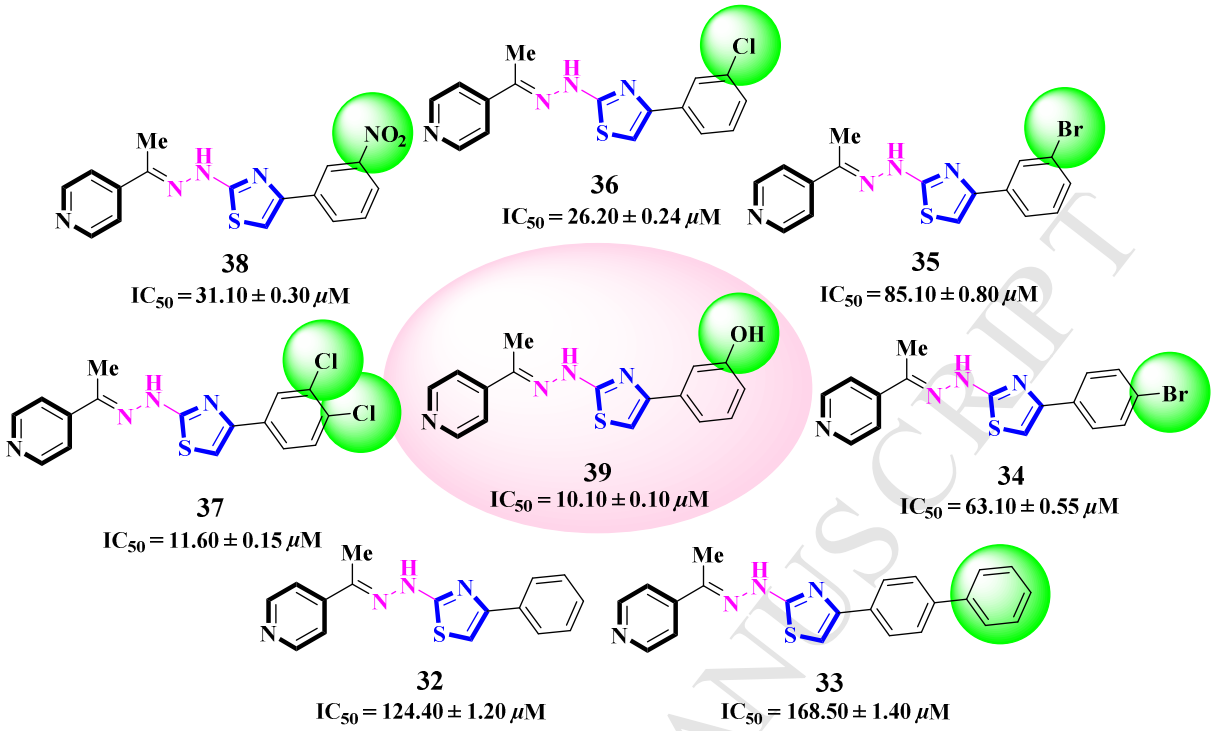

Figure-11: Structure-activity relationship of compounds 32-39

In a nut shell, the whole series was found to be the more potent than standard acarbose. However, the limited structure-activity relationship revealed that the compounds with substituents having more negative inductive effect were found to be more potent than the compounds with the substitutions with less negative inductive effect. To rationalize the interaction of these compounds with the active site of enzyme, *in silico* studies were also carried out.

Molecular docking studies

All synthetic derivatives **1-39** were docked into the binding pocket of *α*-glucosidase enzyme by using the Molecular Operating Environment (MOE) software and Triangular Matching docking method (default). Ten different conformations for each compound were generated. Ligands were allowed to be flexible during the docking in order to acquire the minimum energy structures. Ligands were ranked by the scores from the GBVI/WSA binding free energy calculation in the **S** field by using the software which is the score of the last stage. For all the scoring functions, lower scores show the more favorable pose. The top ranked conformation of each derivative was

selected for further analysis on the basis of docking score (**S**). At the end of docking, the predicted ligand-protein complexes were analyzed for molecular interactions and their 3D images were taken by using LigPlot implemented in MOE.

Interactions details of synthetic compounds

The catalytic site of the modeled α-glucosidase on the basis of the crystallographic structure of *Saccharomyces cerevisiae* isomaltase (PDB code 3AJ7) is composed of Asp214, Glu276, and Asp349 residues. The molecular docking studies also disclosed some other important residues like Pro309, Phe157, Asn347, Arg312, Glu304, His279, and His348 in the α-glucosidase inhibition which showed a slightly different docking profile in the α-glucosidase inhibition. To discuss the interactions details of ligands and protein, all the thirty nine synthesized compounds were classified into four different groups on the basis of their structural similarities. The comparative analysis of ligand-protein interactions for each group was carried out in detail.

Interactions of the hydrazonomethyl pyridine 4-arylthiazole group of compounds

Compounds **1** and **2-12** are classified as hydrazonomethyl pyridine 4-phenylthiazole compounds on the basis of their structural similarities. All these compounds have common hydrazonomethyl pyridine 4-phenylthiazole group in their structures. According to the IC_{50} value, compound **9** (IC_{50} = 6.10 ± 0.01 μM) was the most active compound of this group. Figure-12a showed that compound **9** was well fit into the binding cavity of α-glucosidase showing four interactions with the residues Pro309, Phe157, and Asn347. Pro309 residue is participated in side chain hydrogen donor interaction with the *para*-chlorine of dichlorobenzene. Phe157 showed two π-hydrogen interactions with the π-electrons of dichlorobenzene and thiazole moiety of the compound. Asn347 was found in another π-hydrogen interaction with the π-electrons of terminal pyridine group.

Compound **11** is the second most active compound (IC_{50} = 23.50 ± 0.20 μM) in this group formed three noticeable interactions with the binding site residues Arg312, Glu304, and His348 as displayed in Figure-12b. Arg312 showed π-hydrogen interaction with the pyridine ring of compound.

A side chain hydrogen donor interaction was also percieved between Glu304 and the sulfur of thiazole. The third interaction was backbone hydrogen acceptor interaction between His348 and oxygen of the nitro group of nitrobenzene moiety.

Figure-12c showed that compound **7** (IC_{50} = 28.50 ± 0.25 μM) is forming three interactions with active site residues Asn347, Phe577, and His279. Asn347 was involved in side chain hydrogen acceptor interaction with the nitrogen of hydrazone group. Phe177 showed π-hydrogen interaction with the thiazole group and His279 formed another π-hydrogen interaction with the chlorobenzene ring of the compound.

Compound **8** with IC_{50} value 46.20 ± 0.40 μM is the fourth most active compound in this group and showed two different interactions with the residues Glu276 and His279 as shown in Figure-12d. Glu276 showed a hydrogen donor interaction with the sulfur of thiazole group. His279 was observed in π-hydrogen interaction with the chlorobenzene group.

Structural features such as presence of a group with more negative inductive effect like halogen and nitro (NO_2) groups were found to show good interaction mode and active nature of compound. Among halogens, Cl containing compounds were found superior than Br. Similarly, NO_2 group containing compound (**11**) showed good result than compounds having single Cl/Br. However, compounds containing two Cl groups at *meta-para* position (**8**) showed best interaction mode than nitro containing compound. The brief interaction detail of this group and group **2** *i.e.* compound **1** to **11**, **13** and **22** is given in Table-1S (see the supporting information). In addition to the catalytic residues, molecular docking studies of hydrazonomethyl pyridine 4-phenylthiazole compounds predicted that residues like Pro309, Phe157, Asn347, Arg312, Glu304, His279, and His348 have also played an important role in the α-glucosidase inhibition.

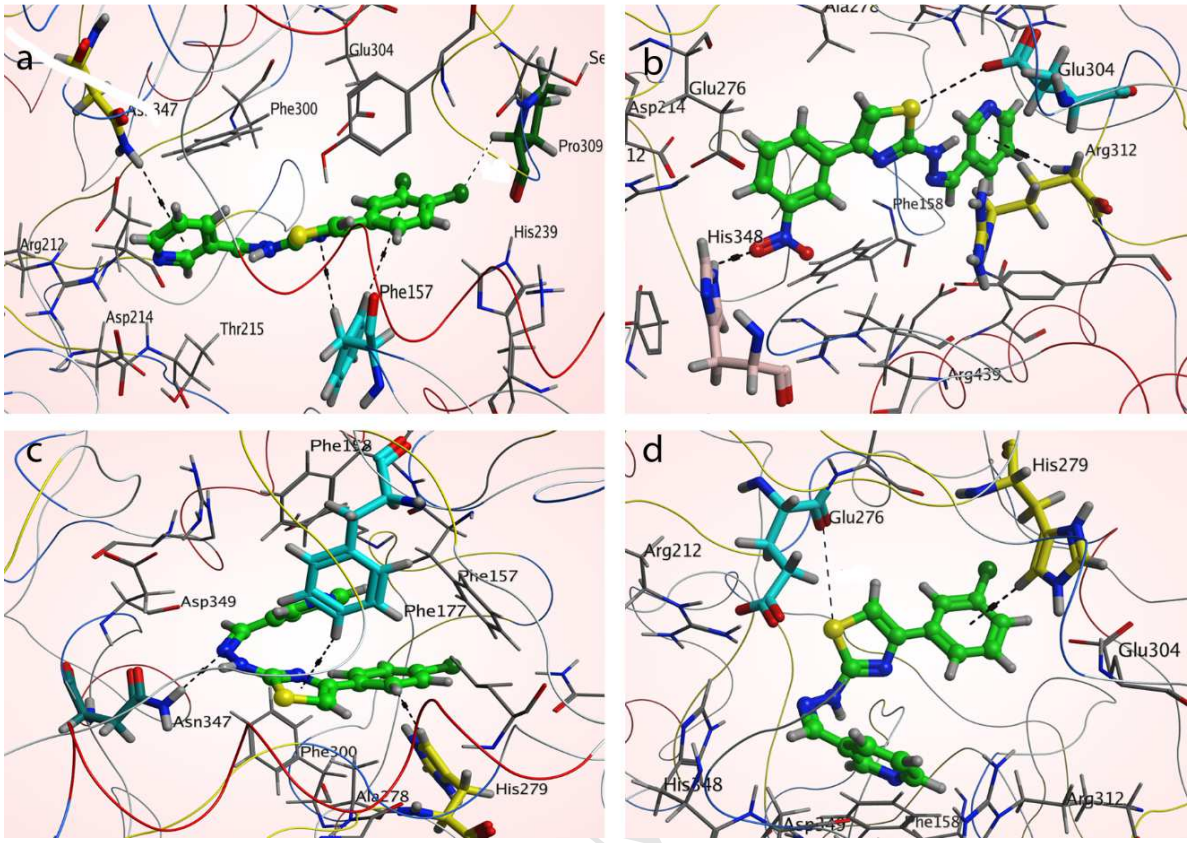

Figure-12: 3D pictures of the docked conformations, (**a**) compound **9**, (**b**) compound **11**, (**c**) compound **7**, and (**d**) compound **8**

Interactions of the hydrazonomethyl pyridine methanethioamide group of compounds

In order to discuss the interaction detail, compounds **1**, **13** and **22** were placed in the second group on the basis of their structural similarity *i.e.* having a common hydrazonomethyl pyridine methanethioamide group. Compound **1** showed two important interactions with the residues Asp349 and His111 (Table-1S). Acidic Asp349 showed a side chain hydrogen donor interaction with nitrogen of thiourea group and His111 formed a hydrogen acceptor interaction with the sulfur of the same group of compound (Table-1S). Compound **13** showed single H-donor interaction with Asp214 using nitrogen of thiourea group. Compound **22**, the most active compound of this group formed three interactions with the residues Asp349, His111, and Phe177 (Table-1S). Asp349 showed H-donor interaction with the nitrogen of thiourea linker and an H-acceptor interaction was observed between the sulfur of thiourea and His111. Whereas, Phe177 formed a π-hydrogen bond with the π system of pyridine moiety of compound (Table-1S). Thiourea group and pyridine with *para* attachment were observed as active moieties in this group

of compounds. Interactions of the hydrazonomethyl pyridine methanethioamide group of compounds predicted the possible inhibitory role of His111 and Phe177 in addition to the catalytic site residues Asp214 and Asp349.

Interactions of the *ortho*-hydrazonoethyl pyridine 4-arylthiazole group of compounds

Compounds **14** to **20** were grouped on the basis of structural similarity in a common hydrazonoethyl pyridine 4-phenylthiazole group. Compound **19** showed highest activity (IC_{50} = 1.40 ± 0.01 μM) in this group as well as in all of the synthesized compounds and showed four important interactions with the residues Asp349, Asn241, His279, and Phe300 as shown in Figure-13a. Asp349 formed H-donor interaction with sulfur of thiazole moiety and a similar interaction was observed between Asn241 and *para*-Cl of dichlorobenzene group of the compound. A π-hydrogen interaction was found between His279 and π system of dichlorobenzene of compound. Another π-hydrogen bond was observed between Phe300 and thiazole ring.

Compound **18** the second most active member (IC_{50} = 5.50 ± 0.10 μM) of this group was found forming three interactions with the residues Asp408, Phe157, and Arg312 as shown in Figure-13b. Acidic Asp408 showed H-donor interaction with sulfur of thiazole group and Phe157 formed π-hydrogen interaction with chlorobenzene ring of the compound. Another π-hydrogen interaction was found between the same chlorobenzene ring and basic Arg312. Compound **20** with IC_{50} value of 13.10 ± 0.15 μM is the third most active compound in this group and showed two different interactions with the residues Glu304 and Phe157 as shown in Figure-13c. Glu304 showed a hydrogen donor interaction with the sulfur of thiazole group. Phe157 was observed in π-π interaction with the nitrobenzene group. Compound **14**, according to IC_{50} value, the fourth member (IC_{50} = 24.10 ± 0.24 μM) of this group showed single H-acceptor interactions with the Asn347 using the lone pair of N of pyridine ring as shown in Figure-13d. The addition of a methyl group adjacent to pyridine ring in the members of this group was observed to improve the interaction mode particularly for the compounds having Cl/NO_2 groups *i.e.* **19**, **18** and **20**. The summary of interactions of compounds of this group and group 4 (**14** to **39**) is given in Table-2S (see the supporting information). The docking profile of the *ortho*-hydrazonoethyl pyridine 4-arylthiazole group of compounds discloses the inhibition role of some additional important residues like Arg312, glu304, Phe157, Asn241, His279, and Phe300, making the target more interesting for further investigation.

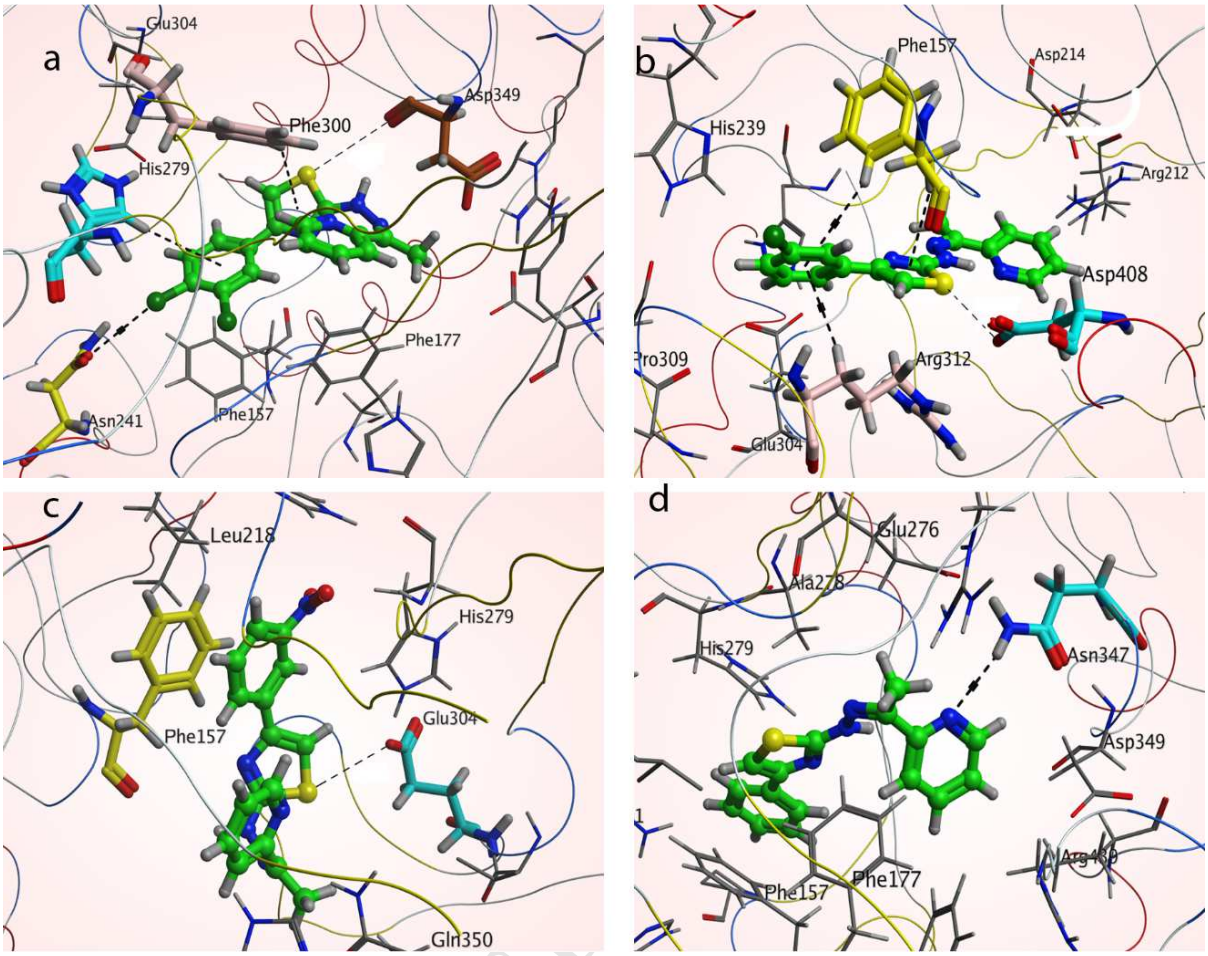

Figure-13: 3D pictures of the docked conformations, (**a**) compound **19**, (**b**) compound **18**, (**c**) compound **20**, and (**d**) compound **14**

Interactions of the *para/meta*-hydrazonoethyl pyridine 4-arylthiazole group of compounds

On the basis of structural similarity in *para/meta*-hydrazonoethyl pyridine 4-phenylthiazole groups, compounds **12**, **21**, **23**, to **39** were grouped together. According to the IC_{50} value, compound **28** (IC_{50} = 2.50 ± 0.01 μM) is the most active compound of this group. It is clear from Figure-14a that compound **28** is showing three interactions in the binding cavity of α-glucosidase with the residues Glu304, Phe157, and Arg312. Glu304 is involved in side chain H-donor interaction with the sulfur of thiazole moiety of compound. Phe157 showed a π-hydrogen interactions with the π-electrons of dichlorobenzene ring of the compound. Arg312 was found in another π-hydrogen interaction with the π-electrons of the same dichlorobenzene group.

Compound **21** with IC_{50} value of 6.40 ± 0.10 μM also showed considerable interactions with the active site residues. The binding mode of compound **28** is shown in Figure-14b. Compound **21**

showed interactions with Asn241, Phe177, and His279. Asn241 formed H-donor interaction with the OH group of phenolic moiety of compound while Phe177 and His279 formed π-hydrogen interactions with the π system of thiazole and phenolic ring, respectively. Comparing the binding mode of compound **21** and **28** it was observed that dichlorobenzene group in compound **28** and phenolic group in **21** imparts almost similar interaction strength *i.e.* one polar and two π-hydrogen interactions. Compound **30**, a *para* analog of compound **21**, showed three π-hydrogen interactions with the active site residues His245, Phe158, and Arg312 as depicted in Figure-14c. His245, Phe158, and Arg312 formed π-hydrogen interactions with the π system of pyridine, thiazole, and phenolic ring, respectively. *Para* attachment of pyridine ring in compound **30** resulted in π-interactions only with no hydrogen bond as compared to compound **21**. The *meta* analog of compound **21** and **30**, compound **39** also showed three interactions, a hydrogen bond and two π-interactions as presented in Figure-14d. Asp408 performed H-donor bonding with the lone pair of sulfur of thiazole. Whereas Phe157 and Arg312 formed π-hydrogen interactions with thiazole and phenolic ring, respectively. In addition to OH and Cl groups, the *para* attachment of pyridine ring in this group of compounds were observed accountable for their good interaction modes. Regarding the binding site residues involved, the docking profile of the *para/meta*-hydrazonoethyl pyridine 4-arylthiazole group of compounds was observed almost similar to the docking profile of hydrazonomethyl pyridine 4-phenylthiazole compounds. The interaction detail given in Table-1S and -2S clearly predict the inhibiting capability of all these synthetic compounds for α-glucosidase enzyme. The docking study of the thirtynine synthetic compounds and the valuable variations of their binding site residues in addition to the catalytic site of the enzyme may lead to further investigate the importance of these very interesting interactions.

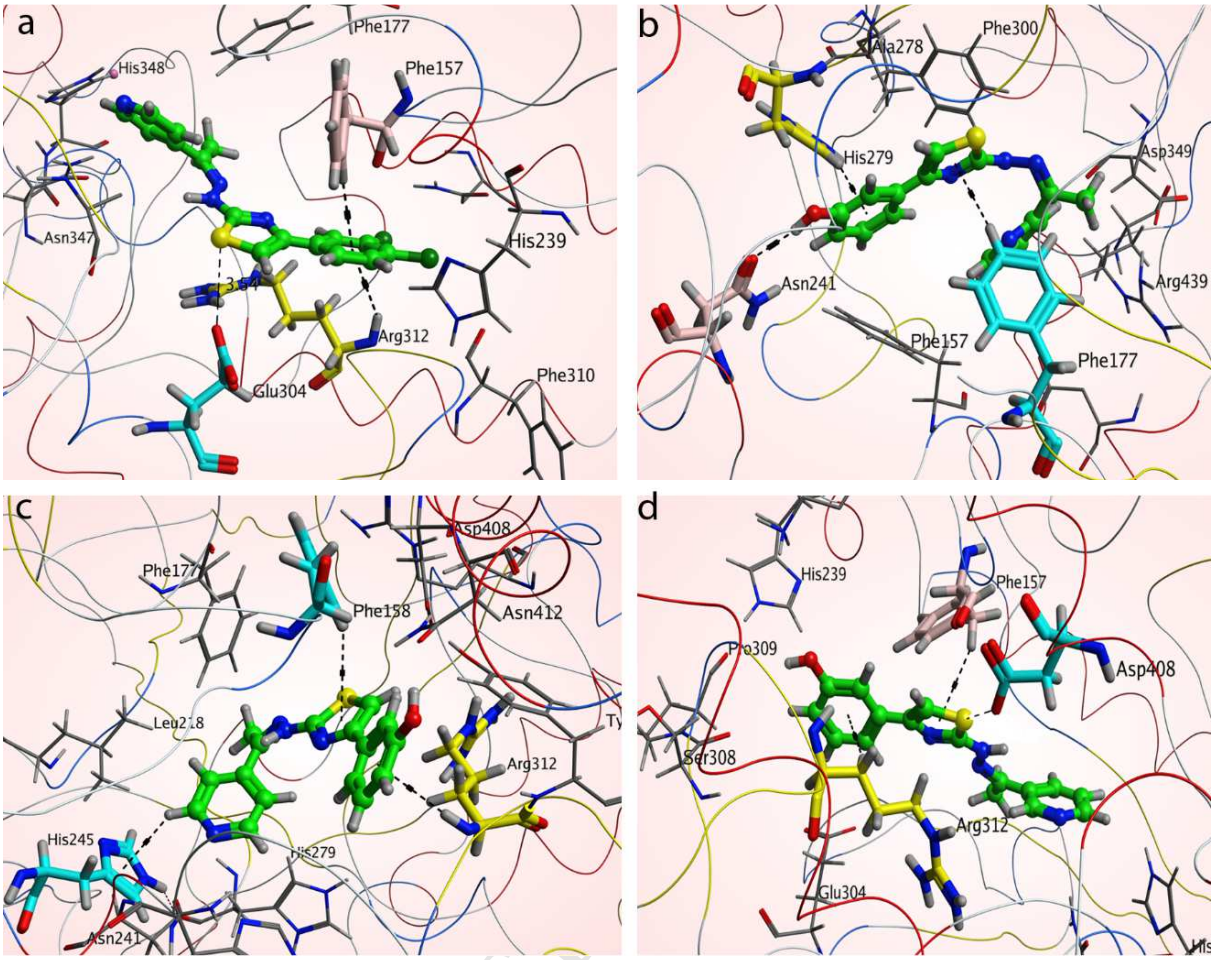

Figure-14: 3D pictures of the docked conformations, (**a**) compound **28**, (**b**) compound **21**, (**c**) compound **30**, and (**d**) compound **39**

Conclusion

Synthetic hydrazinyl arylthiazole based pyridine derivatives **1-39** were screened for α-glucosidase inhibitory activity *in vitro*. All analogs exhibited potent inhibition in the range of IC_{50} = 1.40-236.10 μM as compared to the standard acarbose (IC_{50} = 856.45 ± 5.60 μM). Molecular docking study was conducted to understand the ligand-enzyme interactions and the structure-activity relationship. This study identified a library of lead molecules which can be used in further advance research in order to obtain a powerful inhibitor for α-glucosidase enzyme for the development of insulin-independent antidiabetic agents.

Experimental

Materials and Methods

All reagents and solvents were purchased from Sigma-Aldrich, USA. Thin layer chromatography (TLC) was performed on pre-coated silica gel, GF-254 (Merck, Germany). Spots were visualized under ultraviolet light at 254 and 366 nm. Mass spectra were recorded under on MAT 312 and MAT 113D mass spectrometers. The ^{1}H-, ^{13}C-NMR were recorded on Bruker AM spectrometers, operating at 300, 400 and 500 MHz. The chemical shift values are presented in ppm (δ), relative to tetramethylsilane (TMS) as an internal standard and the coupling constant (J) are in Hz.

General procedure for the synthesis of thiosemicarbazone derivatives of pyridine (1, 13, 22, and 31)

3-Pyridinecarboxaldehyde or 2/3/4-acetylpyridine (10 mmol), thiosemicarbazide (10 mmol) and 2-4 drops of glacial acetic acid in ethanol (10 mL) into a 100 mL round-bottomed flask. Reaction mixture was refluxed for 3 hours. Reaction progress was checked by periodic TLC. After reaction completion, solvent was evaporated and crude product was washed with distilled water and then hexane. Product was crystallized from ethanol.

General procedure for the synthesis of hydrazinyl arylthiazole based pyridine derivatives 1-39

Thiosemicarbazones **1**/**13**/**22**/**31** (1 mmol), phenacyl bromides (1 mmol) and triethyl amine (1 mmol) in ethanol (15 mL) were refluxed for 3 h into a 100 mL round-bottommed flask. Reaction progress was checked by periodic TLC. Precipitates were formed after keeping the flask overnight at room temperature. The solid product was filtered, washed with excess distilled water and dried in vacuum. Product was crystallized from ethanol to afford pure title compounds.

2-(Pyridin-3-ylmethylene)hydrazinecarbothioamide (1)

Yield: 89%; m.p: 227-229 $^{\circ}$C; ^{1}H-NMR (400 MHz, DMSO-d_6) δ 11.55 (s, 1H, NH), 8.91 (d, $J_{2,4}$ = $J_{2,6}$ = 2.0 Hz, 1H, H-2), 8.55 (d, $J_{6,4}$ = 1.6 Hz, $J_{6,5}$ = 4.8 Hz, 1H, H-6), 8.26 (m, 2H, H-4, NH_a), 8.10 (brd.s, 1H, NH_b), 8.05 (s, 1H, H-7), 7.24 (m, 1H, H-5); ^{13}C-NMR (125 MHz, DMSO-d_6): δ 178.2, 150.2, 148.7, 139.2, 133.8, 130.1, 123.7; EI-MS *m/z* (% rel. abund.): 179.9 (M^+, 100),

120.0 (57), 105.0 (74), 76.0 (60), 51.0 (17); HREI-MS Calcd for $C_7H_8N_4S$: *m/z* = 180.0470, Found 180.0477.

4-Phenyl-2-(2-(pyridin-3-ylmethylene)hydrazinyl)thiazole (2)

Yield: 89%; m.p: 204-205 °C; ^{1}H-NMR (400 MHz, DMSO-d_6) δ 12.47 (s, 1H, NH), 8.89 (d, $J_{2,4}$ = 1.6 Hz, 1H, H-2), 8.64 (dd, $J_{6,4}$ = 1.6 Hz, $J_{6,5}$ = 5.2 Hz 1H, H-6), 8.27 (d, $J_{4,5}$ = 8.0 Hz, 1H, H-4), 8.09 (s, 1H, H-7), 7.86 (d, $J_{2",3"} = J_{6",5"}$ = 7.2 Hz, 2H, H-2", 6"), 7.65 (m, 1H, H-5), 7.24 (t, $J_{3''(2'',4'')} = J_{5''(4'',6'')}$ = 7.6 Hz, 2H, H-3′′, 5′′), 7.37 (s, 1H, H-5'), 7.31 (t, $J_{4''(3'',5'')}$ = 7.6 Hz, 1H, H-4′′); ^{13}C-NMR (100 MHz, DMSO-d_6): δ167.8, 146.7, 145.0, 136.9, 135.7, 134.5, 131.7, 128.6, 128.6, 127.6, 125.5, 125.5, 125.1, 117.2, 104.3; EI-MS *m/z* (% rel. abund.): 280.0 (M^+, 68), 176.0 (100), 134.0 (77); HREI-MS Calcd for $C_{15}H_{12}N_4S$: *m/z* = 280.0783, Found 280.0797.

4-(Biphenyl-4-yl)-2-(2-(pyridin-3-ylmethylene)hydrazinyl)thiazole (3)

Yield: 89%; m.p: 203-205 °C; ^{1}H-NMR (300 MHz, DMSO-d_6) δ 12.38 (s, 1H, NH), 8.81 (s, 1H, H-2), 8.56 (d, $J_{6,5}$ = 4.8 Hz, 1H, H-6), 8.07 (ovp, 2H, H-4, 7), 7.95 (d, $J_{2",3"} = J_{6",5"}$ = 8.1 Hz, 2H, H-2", 6"), 7.73 (d, $J_{3",2"} = J_{5",6"} = J_{2''',3'''} = J_{6''',5'''}$ = 8.4 Hz, 4H, H-3", 5", 2′′′, 6′′′), 7.49 (ovp, 4H, H-5', 3′′′, 4′′′, 5′′′), 7.38 (t, $J_{5\,(4,\,6)}$ = 7.2 Hz, 1H, H-5); ^{13}C-NMR (100 MHz, DMSO-d_6): δ168.0, 150.2, 149.5, 147.6, 139.6, 139.1, 138.1, 133.7, 132.9, 130.5, 128.9, 128.9, 127.5, 126.8, 126.8, 126.5, 126.5, 126.1, 126.1, 124.1, 104.2; EI-MS *m/z* (% rel. abund.): 356.0 (M^+, 77), 252.0 (100), 210 (44); HREI-MS Calcd for $C_{21}H_{16}N_4S$: *m/z* = 356.1096, Found 356.1118.

4-(2-(2-(Pyridin-3-ylmethylene)hydrazinyl)thiazol-4-yl)benzonitrile (4)

Yield: 89%; m.p: 252-254 °C; ^{1}H-NMR (300 MHz, DMSO-d_6) δ 12.42 (s, 1H, NH), 8.80 (s, 1H, H-2), 8.55 (d, $J_{6,5}$ = 4.5 Hz, 1H, H-6), 8.07 (s, 1H, H-7), 8.04 (d, $J_{4,5} = J_{2",3"} = J_{6",5"}$ = 8.1 Hz, 3H, H-4, 2′′, 6′′), 7.87 (d, $J_{3",2"} = J_{5",6"}$ = 8.1 Hz, 2H, H-3", 5"), 7.66 (s, 1H, H-5'), 7.45 (m, 1H, H-5), 7.24 (t, $J_{3''(2'',4'')} = J_{5''(4'',6'')}$ = 7.6 Hz, 2H, H-3′′, 5′′), 7.37 (s, 1H, H-5'), 7.47 (m, 1H, H-5); ^{13}C-NMR (100 MHz, DMSO-d_6): δ 168.3, 149.9, 148.8, 147.9, 138.6, 132.6, 132.6, 132.6, 130.1, 126.0, 126.0, 123.9, 118.9, 118.9, 109.6, 107.8; EI-MS *m/z* (% rel. abund.): 305.0 (M^+, 78), 201.0 (100), 159.0 (81),79.0 (9), 51.0 (6); HREI-MS Calcd for $C_{16}H_{11}N_5S$: *m/z* = 305.0735, Found 305.0760.

4-(3-Bromophenyl)-2-(2-(pyridin-3-ylmethylene)hydrazinyl)thiazole (5)

Yield: 89%; m.p: 206-208 °C; ^{1}H-NMR (300 MHz, DMSO-d_6) δ 12.37 (s, 1H, NH), 8.80 (s, 1H, H-2), 8.55 (d, $J_{6,5}$ = 4.2 Hz, 1H, H-6), 8.06 (ovp, 3H, H-4, 7, 6"), 7.86 (d, $J_{4", 5"}$ = 7.5 Hz, 1H, H-4"), 7.51 (s, 1H, H-5'), 7.47 (ovp, 2H, H-2",5"), 7.39 (t, $J_{5\ (4,\ 6)}$ = 7.8 Hz, 1H, H-5); ^{13}C-NMR (125 MHz, DMSO-d_6): δ 168.1, 149.8, 148.8, 147.9, 138.4, 136.8, 132.6, 130.8, 130.2, 130.1, 128.1, 124.3, 123.9, 122.0, 105.6; EI-MS *m/z* (% rel. abund.): 358.1 (M^+, 50), 360.1 (M^+ + 2 , 50), 254.0 (100), 174.0 (100), 51.1 (6); HREI-MS Calcd for $C_{15}H_{11}BrN_4S$: *m/z* = 357.9888, Found 357.9894.

4-(4-Bromophenyl)-2-(2-(pyridin-3-ylmethylene)hydrazinyl)thiazole (6)

Yield: 89%; m.p: 222-224 °C; ^{1}H-NMR (300 MHz, DMSO-d_6) δ 12.36 (s, 1H, NH), 8.80 (s, 1H, H-2), 8.55 (d, $J_{6,5}$ = 4.5 Hz, 1H, H-6), 8.06 (s, 1H, H-7), 8.06 (d, $J_{4,5}$ = 8.4 Hz, 1H, H-4), 7.81 (d, $J_{2", 3"} = J_{6", 5"}$ = 8.4 Hz, 2H, H-2", 6"), 7.60 (d, $J_{3", 2"} = J_{5", 6"}$ = 8.4 Hz, 2H, H-3", 5"), 7.47 (t, $J_{5\ (4,\ 6)}$ = 5.1 Hz, 1H, H-5), 7.43 (s, 1H, H-5'); ^{13}C-NMR (100 MHz, DMSO-d_6): δ 168.1, 149.9, 149.4, 147.9, 138.4, 133.8, 133.8, 132.6, 131.5, 131.5, 130.3, 127.5, 123.9, 120.5, 104.9; EI-MS *m/z* (% rel. abund.): 358.1 (M^+, 52), 360.1 (M^+ + 2, 50), 256.1 (91), 174.1 (100), 79.0 (10); HREI-MS Calcd for $C_{15}H_{11}BrN_4S$: *m/z* = 357.9888, Found 357.9900.

4-(4-Chlorophenyl)-2-(2-(pyridin-3-ylmethylene)hydrazinyl)thiazole (7)

Yield: 89%; m.p: 223-225 °C; ^{1}H-NMR (300 MHz, DMSO-d_6) δ 12.36 (s, 1H, NH), 8.80 (s, 1H, H-2), 8.55 (d, $J_{6,5}$ = 4.5 Hz, 1H, H-6), 8.06 (s, 1H, H-7), 8.06 (d, $J_{4,5}$ = 9.3 Hz, 1H, H-4), 7.87 (d, $J_{2", 3"} = J_{6", 5"}$ = 8.4 Hz, 2H, H-2", 6"), 7.47 (ovp, 4H, H-5, 5', 3", 5"); ^{13}C-NMR (125 MHz, DMSO-d_6): δ, 168.1, 149.8, 149.3, 147.9, 138.3, 133.4, 132.6, 131.9, 130.2, 128.6, 128.6, 127.2, 127.2, 123.9, 104.8; EI-MS *m/z* (% rel. abund.): 314.0 (M^+, 53), 316.0 (M^+ + 2, 20), 210.0 (100), 168.0 (42), 51.0 (7); HREI-MS Calcd for $C_{15}H_{11}ClN_4S$: *m/z* = 314.0393, Found 314.0415.

4-(3-Chlorophenyl)-2-(2-(pyridin-3-ylmethylene)hydrazinyl)thiazole (8)

Yield: 89%; m.p: 202-204 °C; ^{1}H-NMR (300 MHz, DMSO-d_6) δ 12.37 (s, 1H, NH), 8.80 (s, 1H, H-2), 8.55 (d, $J_{6,5}$ = 3.9 Hz, 1H, H-6), 8.06 (ovp, 2H, H-4, 7), 7.89 (s, 1H, H-2"), 7.83 (d, $J_{6", 5"}$ = 7.5 Hz, 1H, H-6"), 7.51 (s, 1H, H-5'), 7.45 (m, 2H, H-4", 5"), 7.40 (t, $J_{5\ (4,\ 6)}$ = 7.8 Hz, 1H, H-5); ^{13}C-NMR (75 MHz, DMSO-d_6): δ 168.1, 149.8, 149.0, 147.9, 138.4, 136.5, 133.4, 132.6, 130.5,

130.2, 127.2, 125.1, 124.0, 123.9, 105.6; EI-MS *m/z* (% rel. abund.): 313.9 (M^+, 47), 315.9 (M^+ + 2 , 18), 209.9 (100), 167.9 (100), 79.0 (6), 51.0 (6); HREI-MS Calcd for $C_{15}H_{11}ClN_4S$: *m/z* = 314.0393, Found 314.0406.

4-(3,4-Dichlorophenyl)-2-(2-(pyridin-3-ylmethylene)hydrazinyl)thiazole (9)

Yield: 89%; m.p: 237-239 °C; ^{1}H-NMR (300 MHz, DMSO-d_6) δ 12.38 (s, 1H, NH), 8.80 (s, 1H, H-2), 8.55 (d, $J_{6,5}$ = 4.5 Hz, 1H, H-6), 8.06 (ovp, 3H, H-4, 7, 2''), 7.85 (dd, $J_{6'', 2''}$ = 1.5 Hz, $J_{6'', 5''}$ = 8.4 Hz, 1H, H-6''), 7.67 (d, $J_{5'', 6''}$ = 8.4 Hz, 1H, H-5''), 7.57 (s, 1H, H-5'), 7.47 (m, 1H, H-5); ^{13}C-NMR (75 MHz, DMSO-d_6): δ 168.2, 149.9, 148.0, 147.9, 138.6, 135.1, 132.6, 131.4, 130.8, 130.2, 129.7, 127.1, 125.5, 123.9, 106.2; EI-MS *m/z* (% rel. abund.): 347.9 (M^+, 83), 349.9 (M^+ + 2 , 71), 243.9 (100), 207.9 (69), 79.0 (10), 51.0 (6); HREI-MS Calcd for $C_{15}H_{10}Cl_2N_4S$: *m/z* = 348.0003, Found 347.9995.

4-(2,4-Dichlorophenyl)-2-(2-(pyridin-3-ylmethylene)hydrazinyl)thiazole (10)

Yield: 89%; m.p: 166-168 °C; ^{1}H-NMR (300 MHz, DMSO-d_6) δ 12.36 (s, 1H, NH), 8.80 (s, 1H, H-2), 8.55 (d, $J_{6,5}$ = 4.2 Hz, 1H, H-6), 8.06 (ovp, 2H, H-4, 7), 7.90 (d, $J_{6'', 5''}$ = 5.4 Hz, 1H, H-6''), 7.69 (d, $J_{3'', 5''}$ = 1.8 Hz, 1H, H-3''), 7.51 (ovp, 3H, H-5, 5', 5''); ^{13}C-NMR (100 MHz, DMSO-d_6): δ167.2, 149.9, 147.9, 138.4, 132.6, 132.5, 132.1, 132.0, 131.5, 130.2, 130.2, 129.7, 127.5, 123.9, 109.5; EI-MS *m/z* (% rel. abund.): 348.0 (M^+, 36), 350.0 (M^+ + 2 , 21), 243.9 (100), 208.0 (37), 79.0 (7), 51.0 (6); HREI-MS Calcd for $C_{15}H_{10}Cl_2N_4S$: *m/z* = 348.0003, Found 348.0003.

4-(3-Nitrophenyl)-2-(2-(pyridin-3-ylmethylene)hydrazinyl)thiazole (11)

Yield: 89%; m.p: 240-242 °C; ^{1}H-NMR (300 MHz, DMSO-d_6) δ 12.47 (s, 1H, NH), 8.81 (s, 1H, H-2), 8.67 (s, 1H, H-2''), 8.56 (d, $J_{6,5}$ = 4.5 Hz, 1H, H-6), 8.31 (d, $J_{4'', 5''}$ = 7.5 Hz, 1H, H-4''), 8.16 (d, $J_{6'', 5''}$ = 8.4 Hz, 1H, H-6''), 8.07 (ovp, 2H, H-4, 7), 7.73 (ovp, 2H, H-5', 5''), 7.47 (m, 1H, H-5); ^{13}C-NMR (100 MHz, DMSO-d_6): δ168.4, 150.0, 148.3, 148.2, 147.9, 138.7, 136.1, 132.7, 131.6, 130.2, 130.2, 124.0, 122.1, 119.9, 106.8; EI-MS *m/z* (% rel. abund.): 325.2 (M^+, 40), 221.1 (100), 175.1 (29), 78.0 (7), 51.0 (6); HREI-MS Calcd for $C_{15}H_{11}N_5O_2S$: *m/z* = 325.0633, Found 325.0647.

3-(2-(2-(Pyridin-3-ylmethylene)hydrazinyl)thiazol-4-yl)phenol (12)

Yield: 89%; m.p: 231-233 °C; ^{1}H-NMR (400 MHz, DMSO-d_6) δ 12.30 (s, 1H, NH), 9.41 (s, 1H, OH), 8.79 (s, 1H, H-2), 8.54 (d, $J_{6,5}$ = 3.6 Hz, 1H, H-6), 8.05 (ovp, 2H, H-4, 7), 7.46 (m, 1H, H-5), 7.27 (ovp, 3H, H-5′, 2″, 6″), 7.19 (t, $J_{5''\,(4'',6'')}$ = 7.6 Hz, 1H, H-5″), 6.70 (d, $J_{4'',\,5''}$ = 8.0 Hz, 1H, H-4"); ^{13}C-NMR (75 MHz, DMSO-d_6): δ 165.8, 152.1; EI-MS *m/z* (% rel. abund.): 296.1 (M^+, 84), 192.0 (100), 164.0 (29), 150.0 (81), 79.1 (20), 51.0 (10); HREI-MS Calcd for $C_{15}H_{12}N_4OS$: *m/z* = 296.0732, Found 296.0720.

2-(1-(Pyridin-2-yl)ethylidene)hydrazinecarbothioamide (13)

Yield: 89%; m.p: 158-160 °C; ^{1}H-NMR (400 MHz, DMSO-d_6) δ 10.28 (s, 1H, NH), 8.56 (d, $J_{6,5}$ = 3.6 Hz, 1H, H-6), 8.41 (d, $J_{3,4}$ = 6.3 Hz, 1H, H-3), 8.37 (s, 1H, NH_a), 8.11 (brd.s, 1H, NH_b), 7.78 (t, $J_{4\,(3,\,5)}$ = 6.0 Hz, 1H, H-4), 7.34 (m, 1H, H-5), 2.37 (s, 3H, C$\underline{H}_3$); ^{13}C-NMR (75 MHz, DMSO-d_6): δ 179.0, 154.6, 148.3, 148.1, 136.3, 123.8, 120.8, 12.0; EI-MS *m/z* (% rel. abund.): 194.1 (M^+, 100), 179.1 (71), 134.1 (59), 106.0 (68), 78.0 (82), 51.0 (26); HREI-MS Calcd for $C_8H_{10}N_4S$: *m/z* = 194.0626, Found 194.0630.

4-Phenyl-2-(2-(1-(pyridin-2-yl)ethylidene)hydrazinyl)thiazole (14)

Yield: 89%; m.p: 125-126 °C; ^{1}H-NMR (400 MHz, DMSO-d_6) δ 11.45 (s, 1H, NH), 8.57 (d, $J_{6,5}$ = 4.0 Hz, 1H, H-6), 8.03 (d, $J_{3,4}$ = 8.4 Hz, 1H, H-3), 7.88 (ovp, 3H, H-4, 2", 6"), 7.42 (ovp, 4H, H-5', 3", 4", 5"), 7.31 (t, $J_{5\,(4,\,6)}$ = 7.6 Hz, 2H, H-5), 2.40 (s, 3H, C$\underline{H}_3$); ^{13}C-NMR (75 MHz, DMSO-d_6): δ 169.3, 154.6, 149.2, 148.3, 138.3, 136.8, 133.7, 129.0, 128.5, 127.5, 125.5, 124.2, 123.4, 104.4, 21.7, 12.2; EI-MS *m/z* (% rel. abund.): 294.1 (M^+, 100), 216.1 (53), 189.1 (85), 134.0 (39), 79.1 (47), 51.0 (10); HREI-MS Calcd for $C_{16}H_{14}N_4S$: *m/z* = 294.0939, Found 294.0927.

4-(Biphenyl-4-yl)-2-(2-(1-(pyridin-2-yl)ethylidene)hydrazinyl)thiazole (15)

Yield: 89%; m.p: 173-176 °C; ^{1}H-NMR (400 MHz, DMSO-d_6) δ 11.47 (s, 1H, NH), 8.58 (d, $J_{6,5}$ = 4.4 Hz, 1H, H-6), 8.04 (d, $J_{3,4}$ = 8.0 Hz, 1H, H-3), 7.98 (d, $J_{2'',\,3''} = J_{6'',\,5''}$ = 8.0 Hz, 2H, H-2", 6"), 7.86 (t, $J_{4\,(3,5)}$ = 8.0 Hz, 1H, H-4), 7.73 (ovp, 4H, H-5, 5′, 3", 5"), 7.49 (ovp, 3H, H-2‴, 4‴, 6‴), 7.38 (t, $J_{3'''\,(4''',5''')} = J_{5'''\,(4''',6''')}$ =7.2 Hz, 2H, H-3‴, 5‴), 2.41 (s, 3H, C$\underline{H}_3$); ^{13}C-NMR (100 MHz, DMSO-d_6): δ 169.4, 154.9, 148.6, 147.0, 139.0, 136.6, 133.9, 128.9, 128.9, 127.5, 126.8, 126.8,

126.4, 126.4, 126.2, 126.1, 126.1, 124.3, 123.4, 119.5, 104.8, 12.3; EI-MS *m/z* (% rel. abund.): 370.2 (M^+, 100), 292.2 (41), 265.1 (69),79.1 (23), 51.0 (5); HREI-MS Calcd for $C_{22}H_{18}N_4S$: *m/z* = 370.1252, Found 370.1226.

4-(3-Bromophenyl)-2-(2-(1-(pyridin-2-yl)ethylidene)hydrazinyl)thiazole (16)

Yield: 89%; m.p: 90-92 °C; ^{1}H-NMR (400 MHz, DMSO-d_6) δ 11.47 (s, 1H, NH), 8.58 (d, $J_{6,5}$ = 4.4 Hz, 1H, H-6), 8.09 (s, 1H, H-2"), 8.03 (d, $J_{3,4}$ = 8.0 Hz, 1H, H-3), 7.89 (d, $J_{6",5"}$ = 7.6 Hz, 1H, H-6"), 7.86 (t, $J_{4\ (3,5)}$ = 8.4 Hz, 1H, H-4), 7.53 (s, 1H, H-5'), 7.49 (d, $J_{4",5"}$ = 8.0 Hz, 1H, H-4"), 7.39 (ovp, 2H, H-5, 5"), 2.40 (s, 3H, C$\underline{H}_3$); ^{13}C-NMR (100 MHz, DMSO-d_6): δ 169.5, 154.8, 148.5, 147.6, 136.5, 130.8, 130.7, 130.1, 128.2, 124.5, 124.3, 123.4, 119.5, 106.0, 105.8, 12.3; EI-MS *m/z* (% rel. abund.): 372.1 (M^+, 92), 374.0 (M^+ + 2 , 100), 296.0 (70), 267.0 (82), 174.0 (M^+ , 49), 79.0 (88), 51.0 (10); HREI-MS Calcd for $C_{16}H_{13}BrN_4S$: *m/z* = 372.0044, Found 372.0076.

4-(4-Bromophenyl)-2-(2-(1-(pyridin-2-yl)ethylidene)hydrazinyl)thiazole (17)

Yield: 89%; m.p: 177-180 °C; ^{1}H-NMR (400 MHz, DMSO-d_6) δ 11.47 (s, 1H, NH), 8.57 (d, $J_{6,5}$ = 4.4 Hz, 1H, H-6), 8.03 (d, $J_{3,4}$ = 8.0 Hz, 1H, H-3), 7.84 (d, $J_{4,3} = J_{2",3"} = J_{6",5"}$ = 8.4 Hz, 3H, H-4, 2", 6"), 7.61 (d, $J_{3",2"} = J_{5",6"}$ = 8.4 Hz, 2H, H-3", 5"), 7.45 (s, 1H, H-5'), 7.37 (t, $J_{5\ (4,6)}$ = 5.6 Hz, 1H, H-5), 2.39 (s, 3H, C$\underline{H}_3$); ^{13}C-NMR (100 MHz, DMSO-d_6): δ 169.4, 154.8, 149.6, 148.5, 138.3, 136.5, 131.5, 131.5, 127.6, 127.6, 124.3, 123.4, 120.5, 119.5, 105.4, 12.2; EI-MS *m/z* (% rel. abund.): 372.1 (M^+, 86), 374.0 (M^+ + 2 , 100), 296.0 (50), 266.9 (84), 174.0 (M^+ , 40), 79.1 (37), 51.0 (8); HREI-MS Calcd for $C_{16}H_{13}BrN_4S$: *m/z* = 372.0044, Found 372.0041.

4-(3-Chlorophenyl)-2-(2-(1-(pyridin-2-yl)ethylidene)hydrazinyl)thiazole (18)

Yield: 89%; m.p: 128-130 °C; ^{1}H-NMR (400 MHz, DMSO-d_6) δ 11.47 (s, 1H, NH), 8.58 (d, $J_{6,5}$ = 4.4 Hz, 1H, H-6), 8.03 (d, $J_{3,4}$ = 8.4 Hz, 1H, H-3), 7.93 (s, 1H, H-2"), 7.85 (ovp, 2H, H-4, 6"), 7.60 (s, 1H, H-5'), 7.46 (t, $J_{5\ (4,6)}$ = 8.0 Hz, 1H, H-5), 7.37 (ovp, 2H, H-4", 5"), 2.40 (s, 3H, C$\underline{H}_3$); ^{13}C-NMR (100 MHz, DMSO-d_6): δ 169.4, 154.8, 149.1, 148.5, 138.3, 136.5, 133.4, 130.5, 127.2, 125.2, 124.2, 124.0, 123.4, 119.5, 106.1, 12.2; EI-MS *m/z* (% rel. abund.): 328.0 (M^+, 100), 330.0 (M^+ + 2 , 38), 250.0 (58), 223.0 (95), 79.0 (76), 51.0 (15); HREI-MS Calcd for $C_{16}H_{13}ClN_4S$: *m/z* = 328.0549, Found 328.0544.

4-(3,4-Dichlorophenyl)-2-(2-(1-(pyridin-2-yl)ethylidene)hydrazinyl)thiazole (19)

Yield: 89%; m.p: 175-178 °C; ^{1}H-NMR (400 MHz, DMSO-d_6) δ 11.49 (s, 1H, NH), 8.58 (d, $J_{6,5}$ = 4.4 Hz, 1H, H-6), 8.12 (d, $J_{2'', 6''}$ = 2.0 Hz, 1H, H-2''), 8.02 (d, $J_{3,4}$ = 8.0 Hz, 1H, H-3), 7.87 (ovp, 2H, H-4, 6''), 7.68 (d, $J_{5'', 6''}$ = 8.4 Hz, 1H, H-5''), 7.60 (s, 1H, H-5'), 7.39 (t, $J_{5\ (4,\ 6)}$ = 5.2 Hz, 1H, H-5), 2.39 (s, 3H, C$\underline{H}_3$); ^{13}C-NMR (125 MHz, DMSO-d_6): δ 169.5, 154.7, 148.5, 147.6, 136.5, 135.2, 131.4, 130.8, 130.7, 127.2, 125.5, 124.3, 123.4, 119.5, 106.7, 12.2; EI-MS *m/z* (% rel. abund.): 362.0 (M^+, 100), 364.0 (M^+ + 2 , 68), 283.9 (69), 256.9 (90), 207.9 (37), 105.0 (29), 79.0 (82), 51.0 (10); HREI-MS Calcd for $C_{16}H_{12}Cl_2N_4S$: *m/z* = 362.0160, Found 362.0155.

4-(3-Nitrophenyl)-2-(2-(1-(pyridin-2-yl)ethylidene)hydrazinyl)thiazole (20)

Yield: 89%; m.p: 245-247 °C; ^{1}H-NMR (400 MHz, DMSO-d_6) δ 11.57 (s, 1H, NH), 8.72 (s, 1H, H-2''), 8.58 (d, $J_{6,5}$ = 4.8 Hz, 1H, H-6), 8.33 (d, $J_{3,4}$ = 8.0 Hz, 1H, H-3), 8.16 (dd, $J_{4'', 2''}$ = 0.9 Hz, $J_{4'', 5''}$ = 8.0 Hz, 1H, H-4''), 8.04 (d, $J_{6'', 5''}$ = 8.0 Hz, 1H, H-6''), 7.86 (t, $J_{4(3,\ 5)}$ = 8.0 Hz, 1H, H-4), 7.73 (ovp, 2H, H-5', 5''), 7.38 (t, $J_{5\ (4,\ 6)}$ = 7.2 Hz, 1H, H-5), 2.41 (s, 3H, C$\underline{H}_3$); ^{13}C-NMR (75 MHz, DMSO-d_6): δ 169.7, 154.8, 148.6, 147.8, 138.4, 136.6, 136.2, 131.5, 130.2, 124.3, 123.5, 122.0, 120.00, 119.6, 107.2, 12.3; EI-MS *m/z* (% rel. abund.): 339.2 (M^+, 100), 261.2 (87), 234.1 (85), 79.1 (96), 51.0 (12); HREI-MS Calcd for $C_{16}H_{13}N_5O_2S$: *m/z* = 339.0790, Found 339.0760.

3-(2-(2-(1-(Pyridin-2-yl)ethylidene)hydrazinyl)thiazol-4-yl)phenol (21)

Yield: 89%; m.p: 226-228 °C; ^{1}H-NMR (400 MHz, DMSO-d_6) δ 11.41 (s, 1H, NH), 9.41 (s, 1H, OH), 8.57 (d, $J_{6,5}$ = 4.4 Hz, 1H, H-6), 8.03 (d, $J_{3,4}$ = 8.0 Hz, 1H, H-3), 7.85 (t, $J_{4\ (3,5)}$ = 8.4 Hz, 1H, H-4), 7.37 (t, $J_{5\ (4,6)}$ = 5.2 Hz, 1H, H-5), 7.34 (ovp, 3H, H-5', 2'', 6''), 7.18 (t, $J_{5''(4'',\ 6'')}$ = 4.0 Hz, 1H, H-5''), 6.71 (d, $J_{4'', 5''}$ = 8.0 Hz, 1H, H-4''), 2.39 (s, 3H, C$\underline{H}_3$); ^{13}C-NMR (75 MHz, DMSO-d_6): δ 165.8, 152.1; EI-MS *m/z* (% rel. abund.): 310.1 (M^+, 100), 232.1 (83), 205.1 (88), 79.1 (35), 51.1 (7); HREI-MS Calcd for $C_{16}H_{14}N_4OS$: *m/z* = 310.0888, Found 310.0874.

2-(1-(Pyridin-4-yl)ethylidene)hydrazinecarbothioamide (22)

Yield: 89%; m.p: 229-231 °C; ^{1}H-NMR (400 MHz, DMSO-d_6) δ 10.39 (s, 1H, NH), 8.57 (d, $J_{2,3}$ = $J_{6,5}$ = 6.0 Hz, 2H, H-2, 6), 8.40 (brd.s, 1H, NH_a), 8.11 (brd.s, 1H, NH_b), 7.89 (d, $J_{3,2}$ = $J_{5,6}$ =6.0 Hz, 2H, H-3, 5), 2.28 (s, 3H, C$\underline{H}_3$); ^{13}C-NMR (100 MHz, DMSO-d_6): δ 179.2, 149.7, 149.7,

145.0, 144.6, 120.6, 120.6, 13.3; EI-MS *m/z* (% rel. abund.): 194.2 (M^+, 81), 179.1 (100), 160.1 (27), 120.1 (22), 78.0 (62), 51.0 (31); HREI-MS Calcd for $C_8H_{10}N_4S$: *m/z* = 194.0626, Found 194.0633.

4-Phenyl-2-(2-(1-(pyridin-4-yl)ethylidene)hydrazinyl)thiazole (23)

Yield: 89%; m.p: 230-232 °C; ^{1}H-NMR (400 MHz, DMSO-d_6) δ 11.54 (s, 1H, NH), 8.61 (d, $J_{2,3}$ = $J_{6,5}$ = 6.0 Hz, 2H, H-2, 6), 7.88 (d, $J_{2'', 3''}$ = $J_{6'', 5''}$ = 7.6 Hz, 2H, H-2", 6"), 7.70 (d, $J_{3,2}$ = $J_{5,6}$ = 5.6 Hz, 2H, H-3, 5), 7.42 (t, $J_{3''(2'', 4'')}$ = $J_{5''(4'', 6'')}$ = 7.6 Hz, 2H, H-3", 5"), 7.39(s, 1H, H-5'), 7.31 (t, $J_{4''(3'', 5'')}$ = 7.2 Hz, 1H, H-4"), 2.32 (s, 3H, C$\underline{H}_3$); ^{13}C-NMR (100 MHz, DMSO-d_6): δ150.8, 150.0, 150.0, 144.8, 143.6, 134.7, 128.6, 128.6, 128.6, 127.6, 125.5, 125.5, 119.7, 119.7, 104.7, 13.37; EI-MS *m/z* (% rel. abund.): 294.0 (M^+, 100), 189.1 (M^+, 32), 175.1 (58), 134.0 (88), 79.0 (34), 51.0 (14); HREI-MS Calcd for $C_{16}H_{14}N_4S$: *m/z* = 294.0939, Found 294.0937.

4-(Biphenyl-4-yl)-2-(2-(1-(pyridin-4-yl)ethylidene)hydrazinyl)thiazole (24)

Yield: 89%; m.p: 277-279 °C; ^{1}H-NMR (400 MHz, DMSO-d_6) δ 11.52 (s, 1H, NH), 8.61 (d, $J_{2,3}$ = $J_{6,5}$ = 4.4 Hz, 2H, H-2, 6), 7.97 (d, $J_{3,2}$ = $J_{5,6}$ = 8.4 Hz, 2H, H-3, 5), 7.73 (ovp, 6H, H-2", 3", 5", 6", 2‴, 6‴), 7.48 (ovp, 3H, H-5', 3‴, 5‴), 7.38 (t, $J_{4''' (3''',5''')}$ = 7.2 Hz, 1H, H-3‴), 2.32 (s, 3H, C$\underline{H}_3$); ^{13}C-NMR (75 MHz, DMSO-d_6): δ169.3, 149.9, 149.9, 149.7, 144.7, 143.6, 139.6, 139.0, 133.8, 128.9, 128.9, 127.4, 126.8, 126.8, 126.4, 126.1, 126.1, 120.6, 119.7, 119.7, 104.9, 13.3; EI-MS *m/z* (% rel. abund.): 370.2 (M^+, 100), 251.2 (M^+, 47), 210.1 (77), 79.1 (14), 51.0 (5); HREI-MS Calcd for $C_{22}H_{18}N_4S$: *m/z* = 370.1252, Found 370.1230.

4-(3-Bromophenyl)-2-(2-(1-(pyridin-4-yl)ethylidene)hydrazinyl)thiazole (25)

Yield: 89%; m.p: 238-240 °C; ^{1}H-NMR (400 MHz, DMSO-d_6) δ 11.56 (s, 1H, NH), 8.61 (d, $J_{2,3}$ = $J_{6,5}$ = 6.0 Hz, 2H, H-2, 6), 8.08 (s, 1H, H-2"), 7.88 (d, $J_{6'', 5''}$ = 7.6 Hz, 1H, H-6"), 7.70 (d, $J_{3,2}$ = $J_{5,6}$ = 6.0 Hz, 2H, H-3, 5), 7.55 (s, 1H, H-5'), 7.50 (d, $J_{4'', 5''}$ = 8.4 Hz, 1H, H-4"), 7.39 (t, $J_{5''(4'', 6'')}$ = 8.0 Hz, 1H, H-5"), 2.32 (s, 3H, C$\underline{H}_3$); ^{13}C-NMR (100 MHz, DMSO-d_6): δ 169.3, 149.9, 149.9, 144.6, 143.8, 136.8, 130.7, 130.0, 128.1, 124.3, 122.0, 120.6, 119.7, 119.7, 106.2, 13.3; EI-MS *m/z* (% rel. abund.): 372.0 (M^+, 90), 374.0 (M^+ + 2, 93), 269.0 (19), 174.0 (100), 78.1 (20), 51.0 (9); HREI-MS Calcd for $C_{16}H_{13}BrN_4S$: *m/z* = 372.0044, Found 372.0045.

4-(4-Bromophenyl)-2-(2-(1-(pyridin-4-yl)ethylidene)hydrazinyl)thiazole (26)

Yield: 89%; m.p: 266-268 °C; ^{1}H-NMR (400 MHz, DMSO-d_6) δ 11.57 (s, 1H, NH), 8.61 (d, $J_{2,3}$ = $J_{6,5}$ = 6.0 Hz, 2H, H-2, 6), 7.83 (d, $J_{2'', 3''}$ = $J_{6'', 5''}$ = 8.8 Hz, 2H, H-2", 6"), 7.99 (d, $J_{3,2}$ = $J_{5,6}$ = 6.4 Hz, 2H, H-3, 5), 7.61 (d, $J_{3'', 2''}$ = $J_{5'', 6''}$ = 8.4 Hz, 2H, H-3", 5"), 7.47 (s, 1H, H-5'), 2.31 (s, 3H, C$\underline{H}_3$); ^{13}C-NMR (75 MHz, DMSO-d_6): δ 169.4, 149.9, 149.9, 144.7, 144.7, 143.7, 133.8, 131.5, 131.5, 127.5, 127.5, 120.5, 119.7, 119.7, 105.5, 13.3; EI-MS *m/z* (% rel. abund.): 372.0 (M^+, 90), 374.0 (M^+ + 2, 93), 174.0 (100), 79.0 (19), 44.0 12); HREI-MS Calcd for $C_{16}H_{13}BrN_4S$: *m/z* = 372.0044, Found 372.0045.

4-(3-Chlorophenyl)-2-(2-(1-(pyridin-4-yl)ethylidene)hydrazinyl)thiazole (27)

Yield: 89%; m.p: 248-250 °C; ^{1}H-NMR (400 MHz, DMSO-d_6) δ 11.56 (s, 1H, NH), 8.61 (d, $J_{2,3}$ = $J_{6,5}$ = 6.0 Hz, 2H, H-2, 6), 7.93 (s, 1H, H-2"), 7.85 (d, $J_{6'', 5''}$ = 7.6 Hz, 1H, H-6"), 7.70 (d, $J_{3,2}$ = $J_{5,6}$ = 6.0 Hz, 2H, H-3, 5), 7.55 (s, 1H, H-5'), 7.46 (t, $J_{5''(4'', 6'')}$ = 7.6 Hz, 1H, H-5"), 7.36 (d, $J_{4'', 5''}$ = 7.6 Hz, 1H, H-4"), 2.32 (s, 3H, C$\underline{H}_3$); ^{13}C-NMR (100 MHz, DMSO-d_6): δ 169.4, 150.0, 150.0, 149.2, 144.7, 143.9, 136.7, 133.5, 130.5, 127.2, 125.3, 124.0, 119.7, 119.7, 106.3, 13.4; EI-MS *m/z* (% rel. abund.): 328.1 (M^+, 100), 330.0 (M^+ + 2, 65), 223.0 (37), 174.0 (53), 78.1 (28), 51.0 (9); HREI-MS Calcd for $C_{16}H_{13}ClN_4S$: *m/z* = 328.0549, Found 328.0577.

4-(3,4-Dichlorophenyl)-2-(2-(1-(pyridin-4-yl)ethylidene)hydrazinyl)thiazole (28)

Yield: 89%; m.p: 261-263 °C; ^{1}H-NMR (400 MHz, DMSO-d_6) δ 11.58 (s, 1H, NH), 8.61 (d, $J_{2,3}$ = $J_{6,5}$ = 6.0 Hz, 2H, H-2, 6), 8.11 (d, $J_{2'', 6''}$ = 2.0 Hz, 1H, H-2"), 7.87 (dd, $J_{6'', 2''}$ = 1.6 Hz, $J_{6'', 5''}$ = 8.4 Hz, 1H, H-6"), 7.69 (ovp, 3H, H-3, 5, 5"), 7.61 (s, 1H, H-5'), 2.32 (s, 3H, C$\underline{H}_3$); ^{13}C-NMR (100 MHz, DMSO-d_6): δ 169.5, 150.0, 150.0, 148.2, 144.7, 144.0, 135.2, 131.4, 130.9, 129.7, 127.2, 125.5, 119.8, 119.8, 107.0, 13.4; EI-MS *m/z* (% rel. abund.): 362.1 (M^+, 100), 364.0 (M^+ + 2, 81), 208.0 (66), 119.1 (18), 78.1 (28), 51.0 (9); HREI-MS Calcd for $C_{16}H_{12}Cl_2N_4S$: *m/z* = 362.0160, Found 362.0188.

4-(3-Nitrophenyl)-2-(2-(1-(pyridin-4-yl)ethylidene)hydrazinyl)thiazole (29)

Yield: 89%; m.p: 258-260 °C; ^{1}H-NMR (400 MHz, DMSO-d_6) δ 11.65 (s, 1H, NH), 8.72 (s, 1H, H-2"), 8.61 (d, $J_{2,3}$ = $J_{6,5}$ = 6.0 Hz, 2H, H-2, 6), 8.32 (d, $J_{4'', 5''}$ = 7.6 Hz, 1H, H-4"), 8.16 (dd, $J_{6'', 2''}$ = 1.6 Hz, $J_{6'', 5''}$ = 8.0 Hz, 1H, H-6"), 7.73 (ovp, 4H, H-3, 5, 5', 5"), 2.33 (s, 3H, C$\underline{H}_3$); ^{13}C-NMR

(100 MHz, DMSO-d_6): δ 169.7, 150.0, 150.0, 148.4, 148.3, 144.7, 144.1, 136.2, 131.5, 130.3, 122.1, 120.0, 119.8, 119.8, 107.4, 13.4; EI-MS *m/z* (% rel. abund.): 339.1 (M^+, 100), 261.1 (M^+, 51), 234.1 (76), 174.0 (80), 78.1 (72), 51.0 (20); HREI-MS Calcd for $C_{16}H_{13}N_5O_2S$: *m/z* = 339.0790, Found 339.0776.

3-(2-(2-(1-(Pyridin-4-yl)ethylidene)hydrazinyl)thiazol-4-yl)phenol (30)

Yield: 89%; m.p: 252-254 °C; ^{1}H-NMR (400 MHz, DMSO-d_6) δ 11.50 (s, 1H, NH), 9.41 (s, 1H, OH), 8.60 (d, $J_{2,3} = J_{6,5}$ = 5.6 Hz, 2H, H-2, 6), 7.69 (d, $J_{3,2} = J_{5,6}$ = 6.4 Hz, 2H, H-3, 5), 7.30 (ovp, 3H, H-5', 2", 6"), 7.20 (t, $J_{5"(4", 6")}$ = 8.0 Hz, 1H, H-5"), 6.71 (d, $J_{4", 5"}$ = 8.0 Hz, 1H, H-4"), 2.31 (s, 3H, C$\underline{H}_3$); ^{13}C-NMR (75 MHz, DMSO-d_6): δ 165.8, 152.1; EI-MS *m/z* (% rel. abund.): 310.1 (M^+, 100), 232.1 (38), 205.1 (34), 150.0 (84), 79.1 (30), 51.0 (12); HREI-MS Calcd for $C_{16}H_{14}N_4OS$: *m/z* = 310.0888, Found 310.0888.

2-(1-(Pyridin-3-yl)ethylidene)hydrazinecarbothioamide (31)

Yield: 89%; m.p: 228-230 °C; ^{1}H-NMR (400 MHz, DMSO-d_6) δ 10.30 (s, 1H, NH), 9.09 (d, $J_{2,4} = J_{2,6}$ = 1.6 Hz, 1H, H-2), 8.55 (dd, $J_{6,2}$ = 1.2 Hz, $J_{6,5}$ = 4.8 Hz, 1H, H-6), 8.32 (ovp, 2H, H-4, NH_a), 8.05 (brd.s, 1H, NH_b), 7.40 (m, 1H, H-5), 2.31 (s, 3H, C$\underline{H}_3$); ^{13}C-NMR (100 MHz, DMSO-d_6): δ 179.1, 149.7, 147.8, 145.6, 133.9, 133.2, 123.2, 13.7; EI-MS *m/z* (% rel. abund.): 194.0 (M^+, 100), 179.0 (46), 120.0 (46), 105.0 (24), 78.0 (71), 51.1 (26); HREI-MS Calcd for $C_8H_{10}N_4S$: *m/z* = 194.0626, Found 194.0638.

4-Phenyl-2-(2-(1-(pyridin-3-yl)ethylidene)hydrazinyl)thiazole (32)

Yield: 89%; m.p: 207-209 °C; ^{1}H-NMR (400 MHz, DMSO-d_6) δ 11.39 (s, 1H, NH), 8.95 (d, $J_{2,4}$ = 0.8 Hz, 1H, H-2), 8.55 (d, $J_{6,5}$ = 4.0 Hz, 1H, H-6), 8.12 (d, $J_{4,5}$ = 8.0 Hz, 1H, H-4), 7.88 (d, $J_{2", 3"} = J_{6", 5"}$ = 7.6 Hz, 2H, H-2", 6"), 7.45 (t, $J_{5(4,6)}$ = 4.8 Hz, 1H, H-5), 7.42 (t, $J_{3"(2",4")} = J_{5"(4",6")}$ = 8.0 Hz, 2H, H-3", 5"), 7.35 (s, 1H, H-5'), 7.31 (t, $J_{4"(3", 5")}$ = 7.6 Hz, 1H, H-4"), 2.35 (s, 3H, C$\underline{H}_3$); ^{13}C-NMR (100 MHz, DMSO-d_6): δ 169.6, 150.8, 149.3, 146.9, 144.1, 134.8, 133.5, 132.8, 128.6, 128.6, 127.5, 125.5, 125.5, 123.5, 104.4, 13.8; EI-MS *m/z* (% rel. abund.): 294.1 (M^+, 100), 175.1 (31), 134.1 (63), 78.1 (23), 51.0 (9); HREI-MS Calcd for $C_{16}H_{14}N_4S$: *m/z* = 294.0939, Found 294.0919.

4-(Biphenyl-4-yl)-2-(2-(1-(pyridin-3-yl)ethylidene)hydrazinyl)thiazole (33)

Yield: 89%; m.p: 245-247 °C; ^{1}H-NMR (400 MHz, DMSO-d_6) δ 11.42 (s, 1H, NH), 8.96 (d, $J_{2,4}$ = 1.6 Hz, 1H, H-2), 8.56 (d, $J_{6,2}$ = 3.6 Hz, 1H, H-6), 8.13 (d, $J_{4,5}$ = 8.0 Hz, 1H, H-4), 7.97 (d, $J_{2",3"}$ = $J_{6",5"}$ = 8.0 Hz, 2H, H-2", 6"), 7.73 (ovp, 4H, H-3", 5", 2‴, 6‴), 7.73 (ovp, 4H, H-5, 5', 3", 5"), 7.38 (t, $J_{4‴\ (3‴,5‴)}$ = 7.2 Hz, 1H, H-4‴), 2.36 (s, 3H, C<u>H</u>$_3$); ^{13}C-NMR (100 MHz, DMSO-d_6): δ 169.6, 150.4, 149.3, 146.9, 144.1, 139.6, 139.0, 133.9, 132.9, 128.9, 128.9, 127.5, 126.8, 126.8, 126.4, 126.4, 126.4, 126.1, 126.1, 123.5, 104.6, 13.8; EI-MS *m/z* (% rel. abund.): 370.2 (M^+, 100), 251.1 (M^+, 54), 210.1 (90), 119.1 (19), 78.1 (24), 51.0 (7); HREI-MS Calcd for $C_{22}H_{18}N_4S$: *m/z* = 370.1252, Found 370.1274.

4-(3-Bromophenyl)-2-(2-(1-(pyridin-3-yl)ethylidene)hydrazinyl)thiazole (34)

Yield: 89%; m.p: 204-205 °C; ^{1}H-NMR (400 MHz, DMSO-d_6) δ 11.41 (s, 1H, NH), 8.95 (s, 1H, H-2), 8.55 (d, $J_{6,5}$ = 4.0 Hz, 1H, H-6), 8.12 (ovp, 2H, H-4, 6"), 7.88 (d, $J_{4",5"}$ = 8.0 Hz, 1H, H-4"), 7.51 (s, 1H, H-5'), 7.49 (ovp, 2H, H-5, 2"), 7.39 (t, $J_{5"(4",\ 6")}$ = 8.0 Hz, 1H, H-5"), 2.35 (s, 3H, C<u>H</u>$_3$); ^{13}C-NMR (100 MHz, DMSO-d_6): δ 169.6, 149.3, 148.9, 146.9, 144.3, 136.9, 133.3, 132.8, 130.7, 130.0, 128.1, 124.3, 123.4, 122.0, 105.9, 13.7; EI-MS *m/z* (% rel. abund.): 372.0 (M^+, 94), 374.0 (M^+ + 2, 94), 174.0 (100), 119.1 (44), 78.1 (52), 51.0 (14); HREI-MS Calcd for $C_{16}H_{13}BrN_4S$: *m/z* = 372.0044, Found 372.0076.

4-(4-Bromophenyl)-2-(2-(1-(pyridin-3-yl)ethylidene)hydrazinyl)thiazole (35)

Yield: 89%; m.p: 244-246 °C; ^{1}H-NMR (400 MHz, DMSO-d_6) δ 11.42 (s, 1H, NH), 8.95 (d, $J_{2,4}$ = 1.6 Hz, 1H, H-2), 8.55 (dd, $J_{6,2}$ = 0.8 Hz, $J_{6,5}$ = 5.2 Hz, 1H, H-6), 8.11 (d, $J_{4,5}$ = 8.4 Hz, 1H, H-4), 7.83 (d, $J_{2",3"}$ = $J_{6",5"}$ = 8.8 Hz, 2H, H-2", 6"), 7.60 (d, $J_{3",2"}$ = $J_{5",6"}$ = 8.8 Hz, 2H, H-3", 5"), 7.45 (ovp, 2H, H-5, 5'), 2.34 (s, 3H, C<u>H</u>$_3$); ^{13}C-NMR (100 MHz, DMSO-d_6): δ 169.7, 149.6, 149.4, 146.9, 144.3, 134.0, 133.4, 132.9, 131.5, 131.5, 127.5, 127.5, 123.5, 120.5, 105.3, 13.8; EI-MS *m/z* (% rel. abund.): 372.0 (M^+, 88), 374.0 (M^+ + 2, 81), 174.0 (100), 119.1 (43), 78.0 (51), 51.0 (17); HREI-MS Calcd for $C_{16}H_{13}BrN_4S$: *m/z* = 372.0044, Found 372.0079.

4-(3-Chlorophenyl)-2-(2-(1-(pyridin-3-yl)ethylidene)hydrazinyl)thiazole (36)

Yield: 89%; m.p: 196-197 °C; ^{1}H-NMR (400 MHz, DMSO-d_6) δ 11.42 (s, 1H, NH), 8.95 (d, $J_{2,4}$ = 1.6 Hz, 1H, H-2), 8.56 (d, $J_{6,5}$ = 4.4 Hz, 1H, H-6), 8.12 (d, $J_{4,5}$ = 8.0 Hz, 1H, H-4), 7.93 (s, 1H,

H-2''), 7.84 (d, $J_{6'',5''}$ = 7.6 Hz, 1H, H-6''), 7.51 (s, 1H, H-5'), 7.45 (ovp, 2H, H-5, 5''), 7.36 (d, $J_{4'',5''}$ = 8.0 Hz, 1H, H-4''), 2.35 (s, 3H, C<u>H</u>$_3$); ^{13}C-NMR (100 MHz, DMSO-d_6): δ 169.7, 149.4, 149.1, 146.9, 144.4, 136.8, 133.5, 133.4, 132.9, 130.5, 127.2, 125.2, 124.0, 123.5, 106.0, 13.8; EI-MS *m/z* (% rel. abund.): 328.1 (M^+, 100), 330.1 (M^+ + 2, 34), 174.1 (38), 119.1 (37), 78.0 (55), 51.0 (14); HREI-MS Calcd for $C_{16}H_{13}ClN_4S$: *m/z* = 328.0549, Found 328.0546.

4-(3,4-Dichlorophenyl)-2-(2-(1-(pyridin-3-yl)ethylidene)hydrazinyl)thiazole (37)

Yield: 89%; m.p: 239-241 °C; ^{1}H-NMR (400 MHz, DMSO-d_6) δ 11.44 (s, 1H, NH), 8.95 (d, $J_{2,4}$ = 1.6 Hz, 1H, H-2), 8.55 (d, $J_{6,5}$ = 3.6 Hz, 1H, H-6), 8.11 (ovp, 2H, H-4, 2''), 7.86 (dd, $J_{6'',2''}$ = 1.6 Hz, $J_{6'',5''}$ = 8.8 Hz, 1H, H-6''), 7.67 (d, $J_{5'',6''}$ = 8.4 Hz, 1H, H-5''), 7.57 (s, 1H, H-5'), 7.46 (m, 1H, H-5), 2.34 (s, 3H, C<u>H</u>$_3$); ^{13}C-NMR (100 MHz, DMSO-d_6): δ 169.8, 149.4, 148.1, 146.9, 144.6, 135.3, 133.3, 132.9, 131.4, 130.9, 129.6, 127.2, 125.5, 123.5, 106.6, 13.8; EI-MS *m/z* (% rel. abund.): 362.1 (M^+, 100), 364.0 (M^+ + 2, 87), 208.0 (46), 119.1 (20), 78.1 (13), 51.0 (4); HREI-MS Calcd for $C_{16}H_{12}Cl_2N_4S$: *m/z* = 362.0160, Found 362.0149.

4-(3-Nitrophenyl)-2-(2-(1-(pyridin-3-yl)ethylidene)hydrazinyl)thiazole (38)

Yield: 89%; m.p: 235-237 °C; ^{1}H-NMR (400 MHz, DMSO-d_6) δ 11.52 (s, 1H, NH), 8.96 (d, $J_{2,4}$ = 1.6 Hz, 1H, H-2), 8.72 (s, 1H, H-2''), 8.56 (d, $J_{6,5}$ = 4.4 Hz, 1H, H-6), 8.32 (d, $J_{4'',5''}$ = 7.6 Hz, 1H, H-4''), 8.15 (ovp, 2H, H-4, 6''), 7.73 (ovp, 2H, H-5', 5''), 7.46 (m, 1H, H-5), 2.36 (s, 3H, C<u>H</u>$_3$); ^{13}C-NMR (100 MHz, DMSO-d_6): δ 169.9, 149.4, 148.3, 148.3, 146.9, 144.6, 136.3, 133.3, 132.9, 131.5, 130.2, 123.5, 122.0, 120.0, 107.1, 13.9; EI-MS *m/z* (% rel. abund.): 339.2 (M^+, 100), 234.2 (46), 174.1 (49), 119.1 (83), 78.1 (94), 51.0 (22); HREI-MS Calcd for $C_{16}H_{13}N_5O_2S$: *m/z* = 339.0790, Found 339.0781.

3-(2-(2-(1-(Pyridin-3-yl)ethylidene)hydrazinyl)thiazol-4-yl)phenol (39)

Yield: 89%; m.p: 202-204 °C; ^{1}H-NMR (400 MHz, DMSO-d_6) δ 11.35 (s, 1H, NH), 9.41 (s, 1H, OH), 8.95 (s, 1H, H-2), 8.55 (d, $J_{6,5}$ = 3.6 Hz, 1H, H-6), 8.11 (d, $J_{4,5}$ = 8.0 Hz, 1H, H-4), 7.45 (m, 1H, H-5), 7.29 (ovp, 3H, H-5', 2'', 6''), 7019 (t, $J_{5''(4'',6'')}$ = 8.0 Hz, 1H, H-5''), 6.70 (dd, $J_{4'',6''}$ = 1.6 Hz, $J_{4'',5''}$ = 8.0 Hz, 1H, H-4''), 2.34 (s, 3H, C<u>H</u>$_3$); ^{13}C-NMR (75 MHz, DMSO-d_6): δ 169.3, 157.5, 149.7, 149.2, 147.7, 146.8, 136.0, 133.4, 132.8, 129.4, 123.4, 116.4, 114.5, 112.4, 104.1, 13.7;

EI-MS *m/z* (% rel. abund.): 310.1 (M^+, 100), 191.1 (35), 150.0 (77), 119.1 (40), 78.1 (52), 51.0 (19); HREI-MS Calcd for $C_{16}H_{14}N_4OS$: *m/z* = 310.0888, Found 310.0909.

Bioassay protocol

***α*-Glucosidase Inhibition Assay**

Baker's Yeast *α*-glucosidase inhibition assay

The enzyme inhibition was carried out according to the protocol previously reported by Taha *et al.* [44]. Test sample (10 μL) was premixed with 50 mM phosphate buffer (95 μL) (pH 6.8), *α*-glucosidase solution (25 μL) (a stock solution of 1 mg/mL in phosphate buffer, was diluted to 0.0625 U/mL with the same buffer just before the assay) and pre-incubated at 37 $^{\circ}$C for 10 min. The reaction was initiated with the addition 5 mM PNPG (25 μL) (dissolve 1.5 mg in 1 mL of phosphate buffer) and absorbance at time 0 minutes was measured. The reaction mixture was then incubated at 37 $^{\circ}$C for 30 min and absorbance at time 30 minutes was measured. For negative control, the test samples were replaced with DMSO (10 μL) and acarbose was used as positive control. The enzymatic hydrolysis of the substrate was monitored based on the amount of *p*-nitrophenol released in the reaction mixture by observation at 405 nm using a microplate reader. All experiments were carried out in triplicate and the results are expressed as the mean ± SD of three determinations.

The percentage (%) inhibition of *α*-glucosidase inhibitory activity was calculated using the equation:

$$\% \text{ Inhibition} = \frac{(A^{30 \text{ minutes}} - A^{0 \text{ minute}})^{\text{control}} - (A^{30 \text{ minutes}} - A^{0 \text{ minute}})^{\text{experiment}}}{(A^{30 \text{ minutes}} - A^{0 \text{ minute}})^{\text{control}}} \times 100$$

Molecular Docking Studies

The 3D structure for *α*-glucosidase of *Saccharomyces cerevisiae* was predicted in this study by using same protocol as described by [45]. The primary sequence of *α*-glucosidase for *Saccharomyces cerevisiae* was retrieved from UniProt (Access code P53341) and template search was performed using Protein BLAST against the PDB. The crystallographic structure of *Saccharomyces cerevisiae* isomaltase (PDB code 3AJ7). Resolution 1.30 Å) with 72.4% of

sequence identity with the target was selected as a template due to its highest sequence identity among the given templates. Ten different models of *α*-glucosidase were generated and refined with AMBER99 forcefield and the best of them was selected and evaluated. The developed model was then subjected to energy minimization up to 0.05 gradients and the quality of the modeled structure was assessed by Ramachandran and ProSA plot. The evaluation of backbone *Psi* and *Phi* dihedral angles for *α*-glucosidase model revealed that 94.8% residues lie in favored region, 4.8% residues lie in allowed region and only 0.3% residues lies in outlier region. Analysis of ProSA shows the Z-value of -10.76 indicating no significant deviation from the score determined for the protein of similar size. The results of both Ramachandran and ProSA plots reflect the accuracy of our modeled structure to be used in docking protocol.

Three dimensional structures of all the compounds were built by using Molecular Builder Module program implemented in MOE and saved as a (mdb) file for molecular docking. Subsequently, the energy of all the compounds was minimized up to 0.05 Gradient using MMFF 94s forcefield implemented in MOE.

Acknowledgement: This work was supported by the Higher Education Commission (HEC) Pakistan (Project No. 20-1910), under the National Research Program for Universities.

References:

1) C. Gao, B. Li, B. Zhang, Q. Sun, L. Li, X. Li, C. Chen, C. Tan, H. Liu, Y. Jiang, Bioorg. Med. Chem. 23 (2015) 1800-1807.
2) H. Gao, Y.N. Huang, P.Y. Xu, J. Kawabata, Food. Chem. 105 (2007) 628-634.
3) F.A. Van de Laar, Vasc. Health Risk Manag. 4 (2008) 1189-1195.
4) R. Rabasa-Lhoret, J.L. Chiasson, R.A. Defronzo, E. Ferrannini, H. Keen, P. Zimmet, *α*-glucosidase inhibitors, International Textbook of Diabetes Mellitus, First ed., John Wiley, UK. 2004.
5) G.S. Meneilly, E.A. Ryan, J. Radziuk, D.C. Lau, J.F. Yale, J. Morais, J.L. Chiasson, R.R. Lhoret, P. Maheux,, D. Tessier, T. Wolever, R.G. Josse, D. Elahi, Diabetes Care, 23 (2000) 1162-1167.
6) L.J. Scott, C.M. Spencer, Miglitol, Drugs, 59 (2000) 521-549.
7) H. AG, Eur. J. Clin. Invest. 24 (1994) 3-10.

8) A.A. Esmaeili, F. Zarifi, A. Moradi, M. Izadyar, and A.R. Fakhari, Tetrahedron Lett. 55 (2014) 333-337.
9) A.R. Katritzky, C.W. Rees, Comprehensive Heterocyclic Chem. Pergamon Press, 1984.
10) G. Hajos, Z. Riedl, G. Kollenz, Eur. J. Org. Chem. 18 (2001) 3405-3414.
11) K.C. Majumdar, P.K. Basu, P.P. Mukhopadhyay, Tetrahedron 60 (2004) 6239-6278.
12) F. Balkenhohl, C. Van dem Bussche-Hunnefeld, A. Lansky, C. Zechel, Ang. Chem. Int. Ed. Eng. 35 (1996) 2288-2337.
13) J.B. Gujar, M.A. Chaudhari, D.S. Kawade, M.S. Shingare, Tetrahedron Lett. 55 (2014) 6939-6942.
14) J.M. Hung, H.J. Arabshahi, E. Leung, J. Reynisson, D. Barker, Eur. J. Med. Chem. 86 (2014) 420-437.
15) D.N.K. Reddy, K.B. Chandrasekhar, Y.S.S. Ganesh, B.S. Kumar, R. Adepu, M. Pal, Tetrahedron Lett. 56 (2015) 4586-4589.
16) A.O. Plunkett, Nat. Prod. Rep. 11 (1994) 581-590.
17) N.D.P. Cosford, L. Tehrani, J. Roppe, E. Schweiger, N.D. Smith, J. Anderson, L. Bristow, J. Brodkin, X. Jiang, I. McDonald, S. Rao, M. Washburn, M.A. Varney, J. Med. Chem. 46 (2003) 204-206.
18) B.C. May, J.A. Zorn, J. Witkop, J. Sherrill, A.C. Wallace, G. Legname, S.B. Prusiner, F.E. Cohen, J. Med. Chem. 50 (2007) 65-73.
19) M. Sridhar, B.C. Ramanaiah, C. Narsaiah, B. Mahesh, M. Kumaraswamy, K.K.R Mallu, V.M. Ankathi, P.S. Rao, Tetrahedron Lett. 50 (2009) 3897-3900.
20) M.T. Cocco, C. Congiu, V. Lilliu, V. Onnis, Eur. J. Med. Chem. 40 (2005) 1365-1372.
21) L.C.W Chang, J.K. von F.D. Künzel, T.M. Krieger, R.F. Spanjersberg, S.F. Roerink, G. van den Hout, M.W. Beukers, J. Brussee, A.P. IJzerman, J. Med. Chem. 48 (2005) 2045-2053.
22) B.B. Fredholm, A.P. IJzerman, K.A. Jacobson, K.N. Klotz, J. Linden, Pharm. Rev. 53 (2001) 527-552.
23) P.V. Kumar, K.M. Reddy, V.R. Rao, Ind. J. Chem. Section B. 47 (2008) 759-763.
24) B. Holla, K. Malini, B. Rao, B. Sarojini, N. Kumari, Eur. J. Med. Chem. 38 (2003) 313-318.
25) N. Siddiqui, M. Arshad, S.A. Khan, Acta. Pol. Pharm. Drug. Res. 66 (2009) 161-167.

26) R. Kalkhambkar, G. Kulkarni, H. Shivkumar, R. Rao, Eur. J. Med. Chem. 42 (2007) 1272-1276.

27) Z. Fan, Z. Shi, X. Liu, Z. Fan, Y. Ai, Faming Zhuanli Shenqing Gongkai Shuomingshu, 2006, 17p. Chinese patent: CNXXEV CN 1810808 A 20060802.

28) F.C. Spector, L. Liang, H. Giordano, M. Sivaraja, M.G. Peterson, J. Virol. 72 (1998) 6979-6987.

29) K.M. Sytnik, I. Ye, S. Bylov, N. Kovalenko, Zhurnal Organichnoi ta Farmatsevtichnoi Khimii, 1 (2003) 71-74.

30) A. Kamal, S.F. Adil, J. Tamboli, B. Siddardha, U. Murthy, Lett. Drug. Des. Disc. 6 (2009) 201-209.

31) H.I. El-Subbagh, H.A. Ashraf, L. Jochen, Archiv der Pharmazie, 332 (1999) 137-142.

32) J. Das, J. Furch, C. Liu, R. Moquin, J. Lin, S. Spergel, K. McIntyre, D. Shuster, K. O'Day, B. Penhallow, Bioorg. Med. Chem. Lett. 16 (2006) 3706-3712.

33) K. Wang, L. Bao, K. Ma, J. Zhang, B. Chen, J. Han, J. Ren, H. Luo, H. Liu, Eur. J. Med. Chem. 127 (2017) 1035-1046.

34) K. Wang, L. Bao, Q. Qi, F. Zhao, K. Ma, Y. Pei, H. Liu, J. Nat. Prod. 78 (2015) 146-154.

35) K. Wang, L. Bao, W. Xiong, K. Ma, J. Han, W. Wang, W. Yin, H. Liu, J. Nat. Prod. 78 (2015) 1977-1989.

36) Q.Q. Tao, K. Ma, L. Bao, K. Wang, J.J. Han, J.X. Zhang, C.Y. Huang, H.W. Liu, Fitoterapia, 111 (2016) 29-35.

37) S.M. Wang, J.J. Han, K. Ma, T. Jin, L. Bao, Y.F. Pei, H.W. Liu, Fitoterapia, 98 (2014) 149-155.

38) K.M. Khan, S. Qurban, U. Salar, M. Taha, S. Hussain, S. Perveen, A. Hameed, N.H. Ismail, M. Riaz, A. Wadood, Bioorg. Chem. 68 (2016) 245.

39) T. Arshad, K.M. Khan, N. Rasool, U. Salar, S. Hussain, T. Tahir, M. Ashraf, A. Wadood, M. Riaz, S. Perveen, M. Taha, N.H. Ismail, Med. Chem. Res. 25 (2016) 2058-2069.

40) M. Taha, N.H. Ismail, S. Lalani, M.Q. Fatmi, Atia-tul-Wahab, S. Siddiqui, K.M. Khan, S. Imran, M.I. Choudhary, Eur. J. Med. Chem., 92 (2015) 387-400.

41) U. Salar, M. Taha, K.M. Khan, N.H. Ismail, S. Imran, S. Perveen, S. Gul, Eur. J. Med. Chem. 122 (2016) 196-200.

42) M. Taha, N.H. Ismail, S. Imran, H. Rashwan, W. Jamil, S. Ali, S.M. Kashi, F. Rahim, U. Salar, K.M. Khan, Bioorg. Chem. 65 (2016) 48-56.

43) H. Niaz, H. Kashtoh, J. AJ. Khan, A. Khan, Atia-tul- Wahab, M.T. Alam, K.M. Khan, S. Perveen, M.I. Choudhary, Eur. J. Med. Chem. 95 (2015) 199-209.

44) M. Taha, N.H. Ismail, S. Imran, M.Q.B. Rokei, S.M. Saad, K.M. Khan, Bioorg. Med. Chem. 23 (2015) 4155-4162.

45) L.R. Guerreiro, E.P. Carreiro, L. Fernandes, T.A. Cardote, R. Moreira, A.T. Caldeira, R.C. Guedes, A. Burke, Bioorg. Med. Chem. 21 (2013) 1911-1917.

Highlights:

- Hydrazinyl arylthiazole based pyridine derivatives **1-39** were synthesized and fully characterized by various spectroscopic techniques.
- All compounds were evaluated for *in vitro* α-glucosidase inhibitory activity.
- All compounds found to be many folds active as compared to the standard acarbose.
- Structure-activity relationship was rationalized by the molecular docking study.